Molecular Neurobiology (2021) 58:5581–5601
https://doi.org/10.1007/s12035-021-02503-w

ORIGINAL ARTICLE

Involvement of TRPM2 in the Neurobiology of Experimental Migraine: Focus on Oxidative Stress and Apoptosis

Yener Yazğan[1] · Mustafa Nazıroğlu[1,2,3,4]

Received: 17 June 2021 / Accepted: 20 July 2021 / Published online: 9 August 2021

Abstract

Excessive Ca^{2+} influx and mitochondrial oxidative stress (OS) of trigeminal ganglia (TG) have essential roles in the etiology of migraine headache and aura. The stimulation of TRPM2 channel via the generation of OS and ADP-ribose (ADPR) induces pain, inflammatory, and oxidative neurotoxicity, although its inhibition reduces the intensity of pain and neurotoxicity in several neurons. However, the cellular and molecular effects of TRPM2 in the TG of migraine model (glyceryl trinitrate, GTN) on the induction of pain, OS, apoptosis, and inflammation remain elusive. GTN-mediated increases of pain intensity, apoptosis, death, cytosolic reactive oxygen species (ROS), mitochondrial ROS, caspase -3, caspase -9, cytosolic Ca^{2+} levels, and cytokine generations (TNF-α, IL-1β, and IL-6) in the TG of TRPM2 wild-type mouse were further increased by the TRPM2 activation, although they were modulated by the treatments of GSH, PARP-1 inhibitors (PJ34 and DPQ), and TRPM2 blockers (ACA and 2APB). However, the effects of GTN were not observed in the TG of TRPM2 knockout mice. The current data indicate that the maintaining activation of TRPM2 is not only important for the quenching OS, inflammation, and neurotoxicity in the TG neurons of mice with experimental migraine but also equally critical to the modulation of GTN-induced pain.

Keywords Apoptosis · Migraine · Oxidative stress · PARP1 · Trigeminal ganglia · TRPM2 channel

Abbreviations

2APB	2-Aminoethoxydiphenyl borate
a.u	Arbitrary unit
ACA	N-(p-amylcinnamoyl)anthranilic acid
Ca^{2+}	Calcium ion
Casp -3	Caspase -3
Casp -9	Caspase -9
CPx	Cumene hydroperoxide
CLSM	Confocal laser scanning microscope
cROS	Cytosolic reactive oxygen species
GSH	Glutathione
GSHPx	Glutathione peroxidase
GTN	Glyceryl trinitrate
MDA	Malondialdehyde
mMP	Mitochondrial membrane potential
mROS	Mitochondrial reactive oxygen species
TG	Trigeminal ganglia
TRPM2	Transient receptor potential 2
OS	Oxidative stress

✉ Mustafa Nazıroğlu
mustafanaziroglu@sdu.edu.tr

[1] Department of Neuroscience, Health Science Institute, Suleyman Demirel University, Isparta, Turkey

[2] Neuroscience Research Center, Suleyman Demirel University, Isparta, Turkey

[3] Drug Discovery Unit, BSN Health, Analyses, Innovation, Consultancy, Organization, Agriculture and Industry Ltd, Isparta, Turkey

[4] Department of Biophysics, Faculty of Medicine, Suleyman Demirel University, TR-32260 Isparta, Turkey

Introduction

Migraine is a common and complex disorder within the human population, and its main symptom is a headache. Within the western countries, the high incidence rate (12%) of the migraine was reported [1]. The incidence rate of migraine is three times higher in women as compared with men [2]. The activations of the trigeminal nerve system and central neuronal current circulation have essential roles in the etiology of migraine [3, 4]. The accumulation evidence indicates that migraine with aura and cortical spreading depression is characterized by the increase of propagating neuronal mitochondrial depolarization [5, 6]. The increase of mitochondrial membrane depolarization is induced by the accumulation of cytosolic free calcium ion (cCa^{2+}) into the

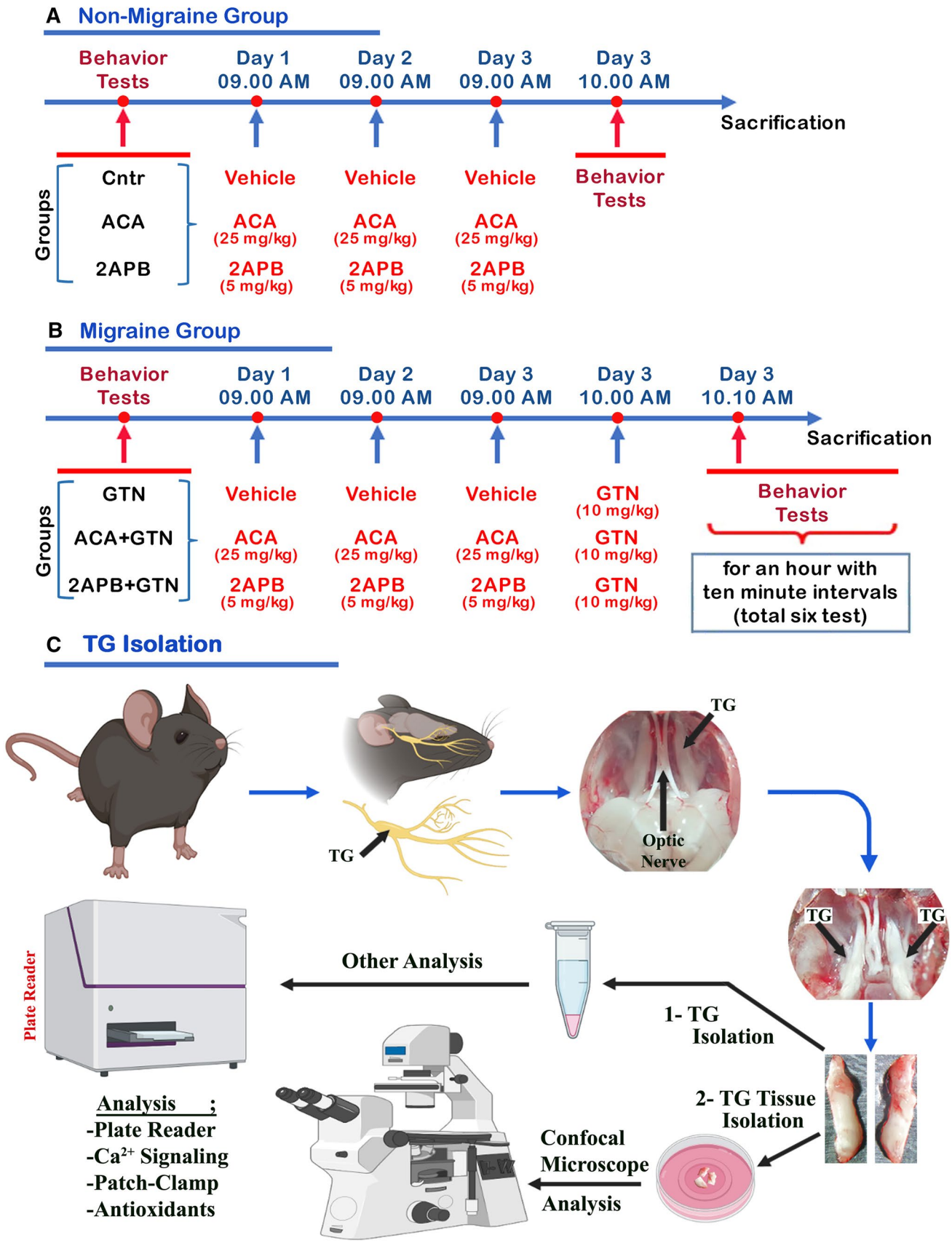
A Non-Migraine Group
Behavior Tests
Day 1 09.00 AM
Day 2 09.00 AM
Day 3 09.00 AM
Day 3 10.00 AM
Sacrification
Groups
Cntr
ACA
2APB
Vehicle
ACA (25 mg/kg)
2APB (5 mg/kg)
Vehicle
ACA (25 mg/kg)
2APB (5 mg/kg)
Vehicle
ACA (25 mg/kg)
2APB (5 mg/kg)
Behavior Tests
B Migraine Group
Behavior Tests
Day 1 09.00 AM
Day 2 09.00 AM
Day 3 09.00 AM
Day 3 10.00 AM
Day 3 10.10 AM
Sacrification
Groups
GTN
ACA+GTN
2APB+GTN
Vehicle
ACA (25 mg/kg)
2APB (5 mg/kg)
Vehicle
ACA (25 mg/kg)
2APB (5 mg/kg)
Vehicle
ACA (25 mg/kg)
2APB (5 mg/kg)
GTN (10 mg/kg)
GTN (10 mg/kg)
GTN (10 mg/kg)
Behavior Tests
for an hour with ten minute intervals (total six test)
C TG Isolation
TG
TG
Optic Nerve
TG
TG
1- TG Isolation
2- TG Tissue Isolation
Other Analysis
Plate Reader
Analysis ;
-Plate Reader
-Ca2+ Signaling
-Patch-Clamp
-Antioxidants
Confocal Microscope
Analysis

◂**Fig. 1 The summary of the study plan and trigeminal ganglia isolation.** (Mean ± STD and n = 10). **a** The behavior tests of mice were performed at basal levels. Then, all mice were divided into two main groups as migraine (GTN) and non-migraine. Lastly, the mice in both groups received TRPM2 channel blockers (ACA, 25 mg/kg and 2APB, 5 mg/kg) for three days. Migraine was induced by a single dose of GTN (10 mg/kg). In non-migraine group, the behavioral tests were performed at 3rd day. **b** In the GTN, ACA + GTN, and 2APB + GTN groups, the behavioral tests were performed at 3rd day for one hour with 10-min intervals (total six tests). At the end of the experiments, all mice were killed, and the whole trigeminal ganglia (TG) neurons were obtained. **c** The whole TG neurons were used for the CLSM-800 microscope analyses. For remaining analyses, TG culture was used by using the centrifugation and collagenase exposure of TGs

mitochondria [7]. It was reported that migraine is associated with the induction of mitochondrial membrane depolarization-induced oxidative stress (OS), inflammation, and apoptosis in the trigeminal nociceptive system [3, 6]. In most subjects, the intake or exposure of glyceryl trinitrate (GTN) caused the induction of typical migraine attacks, including typical severe headaches [7, 8]. The increase of Ca^{2+} influx-mediated OS was reported in the brain and neurons of mice and rats after the treatment of GTN [10–12]. Because of the unclear etiology of migraine, the inhibition of Ca^{2+} influx in the treatment of OS-induced apoptosis is a major limitation.

Migraine-induced headache results in severe pain in the head of patients. In the etiology of several pain diseases such as migraine and headache, the overload Ca^{2+} influx has an essential role [13, 14]. A superfamily for the Ca^{2+} influx is transient receptor potential (TRP) [13, 14]. A member of the TRP superfamily is TRP melastatin 2 (TRPM2). The TRPM2 is stimulated by OS (H_2O_2) and ADP-ribose (ADPR) [15, 16]. TRPM2 was abundantly present in the neurons of pain systems such as dorsal root ganglion (DRG) and trigeminal ganglia (TG) [17, 18]. Hence, TRPM2 is considered a major pain transducer since the inhibition of TRPM2 modulates different types of pain such as neuropathic pain and fibromyalgia [13, 19]. TRPM2 may also attribute to the abnormalities of TGs, since the excessive generations of mitochondrial (mROS) and cytosolic reactive oxygen species (cROS) can target the channel [17]. Furthermore, antioxidants or plant extracts used for the treatment of pain inhibit TRPM2 [19, 20]. In addition to the TRPM2 channels, the TRP ankyrin (A1) and TRP vanilloid 1 TRPV1 channels are activated by mROS and cROS. Involvements of OS-dependent TRPA1 and TRPV1 in the etiology of migraine were recently reported [21]. However, the involvement of TRPM2 for this migraine in experimental animals and humans is unknown.

The death of neurons in pain disorders, including migraine is induced by programmed cell death (apoptosis) [3]. Apoptosis is an ATP-dependent process. Among several pathophysiological pathways of apoptosis in the TGs, the dysfunction of mitochondria is an important molecular pathway [22]. In several neurons, including the TG, mitochondria are involved in the regulation of cCa^{2+} by buffering the TGs against the high amount of cCa^{2+} [23, 24]. Changes in the concentrations of cCa^{2+} may severely affect mitochondrial function, leading to a cascade of OS and caspase events that eventually cause neuronal death [3, 25]. The activation of TRPM2 induced the increase of apoptosis and cell death in the DRGs and sciatic nerve, although its inhibition modulated the increase of apoptosis and cell death in the neurons [18–20]. However, the involvement of TRPM2 on processes of apoptosis and neuronal death in the TGs of mice has not been clarified yet.

The etiology and treatment of migraine were not fully clarified yet. However, migraine is characterized by the excessive Ca^{2+} influx-induced abnormality and neurotoxicity of TG. The excessive generations of mROS and cROS in TGs of patients and rodents with migraine were reported [10, 11, 26]. In several neurons, the exposure of OS directly stimulates the TRPM2 channel, inducing pain, apoptosis, and neurotoxicity [17–19]. However, there is no report on the changes of TRPM2 activity in the TG neurons and experimental GTN migraine model. We hypothesized the investigate these issues in the experimental GTN migraine mouse model. The first aim of the current study was to determine the effect of TRPM2 activation on the value of pain induction, apoptosis, neuronal death, cytokine generation, and mROS in the TGs of mouse with experimental migraine. The second aim of this investigation was to establish the molecular protective response of TRPM2 blocker treatments to the values in the TGs.

Material and Methods

Animals

In the current study, we used 80 TRPM2 wild type ($TRPM2^{WT}$) and TRPM2 knock out ($TRPM2^{KO}$) C57BL/6j black mice. The $TRPM2^{KO}$ black mice were obtained from Professor Makoto Tominaga (NIPS, Aichi Okazaki, Japan). Because of the absence of wild type C57BL/6j black mice in the Suleyman Demirel University (SDU), Isparta, Turkey, the ethical approve of the black mice was taken from Burdur Mehmet Akif University (BMAU), Turkey and they were purchased from the BMAU. The mice were kept in plastic cages under standard ambient temperature (23 ± 1 °C) and 12 h dark/light cycle with free access to food and water.

Study Groups

Before starting the treatments, the tests of behavior were performed in the mice at the basal level. Then, the mice were divided into two main groups as migraine (GTN) and

non-migraine (Figs. 1a and b). Both groups were divided into the six subgroups as follows:

Control group: Mice in the group have not received the treatments of GTN, N-(p-amylcinnamoyl)anthranilic acid (ACA), and 2-aminoethoxydiphenyl borate (2APB).

ACA group: Mice in the group were intraperitoneally treated with ACA [25 mg/kg body weight (B.W.)] for 3 days (total three doses) [27].

2APB group: Mice in the group were intraperitoneally treated with 2APB (5 mg/kg B.W.) for 3 days (total three doses) [28].

Migraine (GTN) group: Mice in the group were intraperitoneally treated with a single dose of GTN (10 mg/kg B.W.) for the induction of migraine [8, 10, 11].

ACA + GTN group: Mice in the group were treated with ACA (25 mg/kg B.W.) for 3 days, and then, they were further treated with a single dose of GTN.

2APB + GTN group: Mice in the group were treated with 2APB (5 mg/kg B.W.) for 3 days, and then they were further treated with a single dose of GTN.

In addition to the six groups, we induced a GSH treatment group. In the groups, the mice were intraperitoneally treated with glutathione (GSH) (200 mg/kg B.W.) for 14 days [29]. Then, they were further treated with a single dose of GTN.

After performing the behavioral tests, all mice were sacrificed under Xylazine and Ketamine anesthesia. The TG was removed for the present analyses.

Pain Sensitivity Tests

In the group of non-migraine, the behavioral tests were performed at the basal level and 3rd day of the treatments (sham, ACA, and 2APB). In the groups of GTN treatments (GTN, ACA + GTN, and 2APB + GTN), the behavioral tests were performed at the basal levels, and then, the tests were repeated at end of the treatments (3rd day) for 1 h and 10-min intervals (total six tests). At the end of the experiments, all mice were killed using the anesthesia of xylazine and ketamine. The mechanical (von Frey) and heat (hot plate) hyperalgesia tests in the paws of mice were performed before starting the treatments (between 8:30 and 9.00 a.m). The analyses of mechanical hyperalgesia in the mice were measured by using the calibrated 20PC Aesthe von Frey filaments (Muromachi Kikai Ltd. Tokyo, Japan) as described in a previous study [19]. The evaluation of the thermal nociceptive threshold in the mouse of each group was performed by using the hot plate test [19]. The pictures of Von Frey needles (Fig. 2a), setup of the Von Frey (Figs. 2b), and hot plate tests (Fig. 2c) are shown in the Fig. 2.

Preparation of TGs

After killing the animals via taking heart blood, the heads of mice were separated. The skull of mice was properly opened and the brain was smoothly taken. Right and left TGs of the mice within the skull bone were separated (Fig. 1). The obtained whole TGs were used for the analyses of antioxidant (spectrophotometer) and confocal laser scanning microscope (CLSM-800) imaging (LSM800, Zeiss, Ankara, Turkey). For the spectrofluorometer (Fura-2), electrophysiology (patch-clamp), and plate reader analyses, TGs were exposed to the further procedures as described in a previous study [3]. Briefly, the removed TGs were exposed to trypsin type III enzyme and 0.5 mg/ml type XI collagenase (Sigma-Aldrich) in 5-ml DMEM medium at 37 °C in a shaking bath for 45 min. The enzymatic digestion of trypsin was stopped by using the soybean trypsin inhibitor (1.25 mg/ml, type II-S1, Sigma-Aldrich). After dissociation with a sterile syringe and centrifugation at 1500 g, the DMEM medium was removed, and the neurons were seeded on the sterile 25 T flasks with filter caps (1×10^3 neurons). The TGs were cultured in the DMEM-LPXA with low glucose (1 g/l) (Capricorn Scientific GmbH, Ebsdorfergrund, Germany), because the high glucose (4.5 g/l) content of the cell culture medium induces TRPM2 activation in neuronal cells [30].

The cCa^{2+} Concentration Determination in the TGs of $TRPM2^{WT}$ and $TRPM2^{KO}$ Mice by Using the stains of Fura-2-AM and Fluo-3-AM

The cCa^{2+} concentration of TGs was performed in a spectrofluorometer (Carry Eclipse, Varian Inc, Ankara, Turkey) and CLSM-800 by using the florescent stains of Fura-2-AM (Molecular Probes Inc., Oregon, USA) and Fluo-3-AM (Calbiochem, Darmstadt, Germany) [19]. The TGs were incubated with the Fura-2-AM (4 µM) and Fluo-3-AM (1 µM) for 45 min. Then, the TGs were washed twice with standard extracellular buffer with 1.2 mM Ca^{2+}. The fluorescence intensities of Fura-2-AM-loaded neurons were monitored in the spectrofluorometer (Carry Eclipse). The excitation wavelengths of Fura-2-AM were kept as 340 and 380 nm, although the emission wavelength was kept as 505 nm. During the Fura-2-AM analyses, the TGs were stirred in the cuvette of spectrofluorometer by magnetic stirrers and temperature (37 °C). The changes of integral rises in the concentrations of cCa^{2+} were recorded in a computer by using a specific program (Carry Eclipse) for 220 s after the addition of cumene hydroperoxide (CPx and 1 mM). The cCa^{2+} concentration is represented as nanomolar (nM) taking a sample every second.

The Fluo-3-AM was excited the CLSM-800 by a 488 nm argon laser. The TGs were treated with TRPM2 channel blockers (100 µM 2APB for 30 min) and PARP1 inhibitors

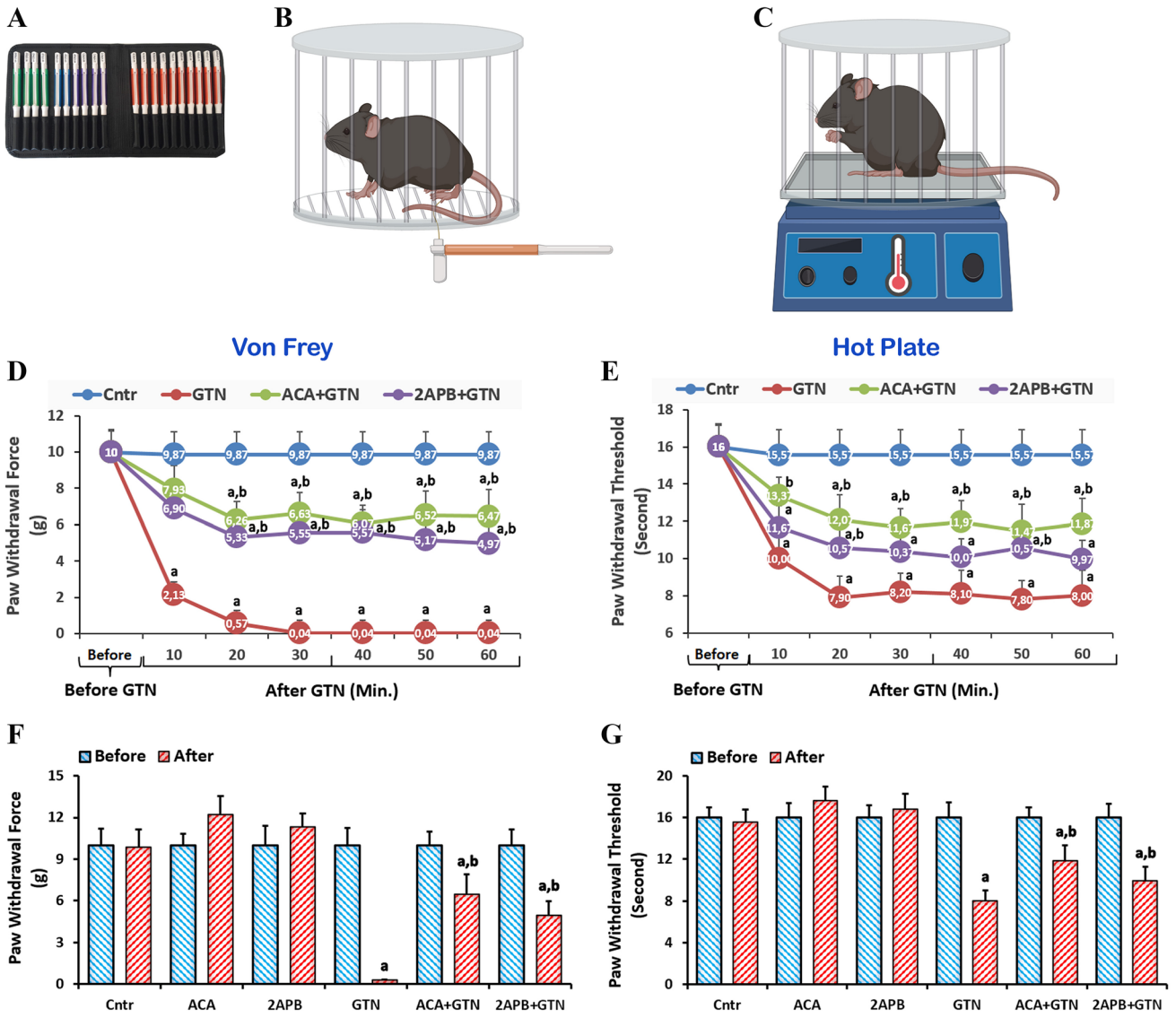

Fig. 2 The effect of TRPM2 channel blocker treatments on paw withdraw threshold of withdrawal force of Von Frey and Hot plate tests in the migraine (GTN)-induced mice. ($n = 10$ and mean ± STD). The von Frey filaments (**a**), von Frey set up (**b**), and hot plate set up (**c**) were used for the hyperalgesia tests. The mean changes of Von Frey were indicated by lines (**d and e**) and columns (**f and g**). ($^{a}p \leq 0.05$ vs the groups of basal, Cntr, ACA, and 2APB groups. $^{b}p \leq 0.05$ *vs* the groups of GTN)

(30 µM DPQ and 1 µM PJ34 for 30 min) to inhibit Ca^{2+} entry before the stimulation of TRPM2 (H_2O_2 and 1 mM). The fluorescence intensities of Fluo-3-AM were analyzed in the CLSM-800 fitted with a 40 × oil objective at 515 nm. The results of Fluo-3-AM in 10 µ m^2 of cytosol were represented as arbitrary unit (a.u.) per cell.

Electrophysiology in the TGs of $TRPM2^{WT}$ and $TRPM2^{KO}$ Mice

The patch-clamp records at whole cell configuration were recorded in a HEKA EPC 10 amplifier (Lamprecht, Germany) by using Patch-master software. Voltage-clamp configuration at -65 mV was induced, and currents were recorded. The content details of intracellular and extracellular buffers were indicated in previous studies [18–20]. In addition to the extracellular ACA (25 µM), the currents of TRPM2 were blocked by using Na^+ free patch chamber solution (*N*-methyl-D-glucamine, $NMDG^+$). The patch pipettes with 5 ± 5 MΩ resistances were produced in a P-97 puller (Sutter Instrument Lab, Ankara, Turkey) from borosilicate glass pipettes. The TGs were stimulated by the cytosolic (via patch-pipette) ADPR (1 mM). The densities of currents in the TGs were expressed as pA/pF.

Live (Hoechst)/Death (PI) Analyses

The florescent probe, propidium iodide (PI), is permeable to the nucleus of death cells, and it represents red color in the nucleus of death cells. The florescent stain, Hoechst, is permeant to the nucleus of live cells, and its blue color image is commonly used to detect live cells in a population. The images of death TG rate (red/blue) and bride field (black/white) in the CLSM-800 microscope fitted with a 40 × oil objective were captured by using the stains of Hoechst and PI [31]. After the incubation of the isolated whole TGs in the DMEM medium, they were further incubated for 30 min with the mixture of Hoechst 33,342 (1 µM) and PI (5 µg/ml) (Cell Signaling Technology, Danvers, MA, USA). The death TGs in the captured images were counted by using the ImageJ/Imaris software. The results of death TG rate are shown as %.

Cell Viability

For assay of cell viability in the TGs, we used common manual method of 4,5-Dimethylthiazol-2-yl)-2,5-diphenyltetrazolium bromide (MTT) [19, 20]. Briefly, the TGs in the black plates were incubated for 4 h at 37 °C to allow the MTT tetrazolium compound to convert into a colored soluble formazan. The absorbance optic densities of MTT were recorded at 490 nm by using a microplate reader (Infinite PRO 200; Tecan Austria GmbH, Groedig, Austria).

The Analyses of Caspase-3 (Casp -3), Caspase-9 (Casp -9), and Apoptosis

The activities of Casp -3 and -9 in the TGs were analyzed from the cleavage of the specific fluorogenic substrates (Ac-DEVD-AMC for CASP-3 and Ac-LEHD-AMC for CASP-9) (Bachem, Bubendorf, Switzerland). The 360 nm was used as excitation wavelength in the Infinite PRO 200, although 460 nm was used as the emission wavelength [32].

The detecting apoptosis as loss of asymmetry in the membranes of apoptotic TGs was measured in the microplate reader (Infinite PRO 200) following the manufacturer's instructions (Biocolor Ltd. Northern Ireland) [32].

The data of Casp -3, Casp -9, and apoptosis were presented as fold increase (experiment/control).

The Measurements of mROS and cROS in the Microplate Reader and CLSM-800 Microscope

The visualization of mROS generation was performed in the CLSM-800 by using 100 nM MitoTracker Red CM-H2Xros fluorescent stain (Life Technologies) [33]. The whole TGs were incubated with the stain of mROS for 30 min at 37 °C in the dark conditions. The stain was excited in the CLSM-800 with a diode laser at 561 nm (Excitation: 576 nm; Emission: 598 nm).

For assaying cROS generation in the captured images of whole TGs, the dihydro-rhodamine 123 (DHR123) and 2′,7′-dichlorofluorescin diacetate (DCFH-DA) probes were used. The DHR123 and DCFH-DA non-fluorescent stains are oxidized to fluorescent intercalators [rhodamine 123 (Rh123) and 2', 7' –dichlorofluorescein (DCF)] by superoxide radicals [34, 35]. After the incubation of the whole TGs with 2 µM DHR123 and DCFH-DA for 25 min at dark, they were washed with 1xBPS, and then they were excited with a diode laser at 488 nm. The fluorescence intensities of Rh123 and DCF in the twenty image fields for each treatment were measured in the CLSM-800 by using the ZEN program, and the results were expressed as a.u.

The analyses of DCFH-DA were repeated in the microplate reader. For the aim, the TGs (1×10^3 TGs/ml DMEM medium) were first incubated in the presence of 2 µM DCFH-DA for 30 min at dark. At the end of DCFH-DA washing, the kinetics of DCF fluorescence intensity (Excitation: 488 nm. Emission: 543 nm) resulting from oxidation of DCFH-DA were measured in the plate reader. The results of Rh123 in the microplate reader were expressed fold increase.

In the dishes with glass bottom, the images of Rh123 and DCF were captured in the CLSM-800 microscope fitted with the oil objective (40x) [33]. The stains of DHR123 and DCFH-DA were excited at 488 nm with a diode laser. The excitation/emission ratio of the fluorescent intensity in the analyses of Rh123 was kept at 507/529 nm, although the ratio was 504/525 nm in the analyses of DCF. The results of DCF and RH123 were indicated as a.u.

The Measurement of Mitochondrial Membrane Potential (mMP) Levels by Using the Microplate Reader and CLSM-800 Microscope

The levels of mMP were assayed in the microplate reader by using a florescent stain (JC1, Cayman Inc. Istanbul, Turkey). The whole TG nerves were incubated in the DMEM medium of the glass bottom dishes for the CLSM-800 analyses, although TGs (10^3) were incubated in the medium of black 96-well plate for the microplate analyses. The JC1 (2 µM) was added to the culture medium of TGs, and it was incubated for 30 min at 37 °C and dark, and then, the TGs in the dishes and black plates were washed three times with 1xBPS.

In the CLSM-800 analyses, the stain of JC1 was excited with a diode laser at 561 nm, and the orange images of JC1 were captured in twenty randomly selected microscopic field areas for each treatment [32, 33]. They were calculated by using the ZEN program. The results of JC1 in the CLSM-800 analyses were indicated as a.u.

In the plate reader JC1 analyses, the kinetic ratio of the fluorescent intensity obtained by the excitation (578 nm)/emission (599 nm) to the fluorescent intensity obtained by the excitation (485 nm)/emission (535 nm) was calculated to quantitate JC1 florescence intensity [32, 33]. After calculating protein levels of the TGs, the mMP results in the analyses of the microplate reader were expressed as fold increase (experiment/control).

Cytosolic GSH Imaging

The concentrations of the cytosolic GSH in the captured GSH images were measured in the CLSM-800 by using a ThiolTracker Violet commercial kit (# T10095, Thermo Fisher Sci., Istanbul, Turkey) according to the procedure of company. The excitation (404 nm) and emission (526 nm) wavelengths of the analyses in the CLSM-800 were used after the laser stimulation (405 nm) [32, 33]. After measuring the florescence intensity in each TG by using the ZEN program, the mean results of the GSH concentration were expressed as a.u.

The Analyses of Lipid Peroxidation (Malondialdehyde, MDA), GSH, and Glutathione Peroxidase (GSHPx) in the TG Homogenate

The optic density (absorbance) values of total protein, MDA, GSH, and GSHPx in the TGs homogenate samples were measured by using the spectrophotometer (Shimadzu-UV1800). The extraction and wavelength details of analyses were indicated in our studies [10, 11, 33]. The unit of μmol/g protein was used in the TGs for the expression of the MDA and GSH levels. The activity of GSHPx in the TGs was expressed as IU/ g protein.

The Analyses of Cytokines by Using the Enzyme-Linked Immunosorbent Assay

The supernatants from the TGs of wild-type mice were collected by the centrifugation (at 1500 g for 5 min). The concentrations of TNF-α (Cat #: E0117Mo), IL-1 β (Cat #: E0045Mo), and IL-6 (Cat #: E0049Mo) were assayed in the Infinite 200 PRO at 450 nm wavelength by using the commercial enzyme-linked immunosorbent assay kit (BTLAB, China) [33]. After the calculation of TNF-α, IL-1β, and IL-6 concentrations from the standard curves, their concentrations were expressed as % of control.

Statistical Analysis

The present data are indicated as means ± standard deviation (STD). The current data were analyzed by using SPSS program (Version 17.0). For the detection of statistical significance, the analyses of One-way ANOVA were used to analyze all data. Significant differences ($p \leq 0.05$) among the values were interpreted using the Tukey's HSD post hoc test.

Results

The Effects of TRPM2 Antagonists (ACA and 2APB) on Mechanical and Thermal Hyperalgesia in GTN-Induced Mice

The hyperalgesia tests (von Frey and hot plate) were performed at basal levels in all mice. Then, all mice were divided into two main groups as non-migraine (control) and migraine (GTN) model. The two main groups were divided into three subgroups as control/GTN, control/ACA + GTN, control/2APB + GTN groups, and the subgroups received the treatments of ACA or 2APB for 3 days. At the end of the treatments, the tests of hyperalgesia in the six groups were repeated six times with 10-min intervals. The figures of the von Frey needles, von Frey setup, and hot plate setup were indicated in the Figs. 2a, b, and c, respectively. There were no changes on the hyperalgesia test results in the groups of Cntr, Cntr + ACA, and Cntr + 2APB (Figs. 2d and e). However, there was a significant decrease in the mechanical withdrawal threshold of the paw bilaterally, which continued to gradually decrease until the 3rd day in all periods analyzed, as indicated by von Frey (Figs. 2d and f) and hot plate (Figs. 2e and g) hyperalgesia assessments ($p \leq 0.05$). In the ACA + GTN and 2APB + GTN groups, the mechanical and heat hyperalgesia results were increased as compared to only GTN group ($p \leq 0.05$). According to the hyperalgesia test results, pretreatment with the TRPM2 channel blockers caused a marked increase in the sensitivity threshold to the mechanical and thermal stimulus ($p \leq 0.05$).

The Treatments of TRPM2 Antagonists (ACA and 2APB) Modulated Cell Death, Apoptosis, Cell viability, Caspase activity, and Lipid Peroxidation via Upregulation of GSH and GSHPx Levels

Current literature data indicate that the depletion of GSH and the increase of OS via the activation of TRPM2 induce neuronal death in several neurons [33, 36–40], although there is no report of TRPM2 via the inhibition of GSH on the neurotoxicity and neuronal death in the TG of migraine-induced animals and human. After observing the decrease of pain sensitivity in the migraine-induced mice by the TRPM2 agonist treatment, we suspected the involvement of TRPM2 via the decrease of GSH level in the migraine-induced mice. We imaged TG death and cytosolic GSH concentration in the CLSM-800 analyses by using the PI/Hoechst stains and GSH commercial kit (ThiolTracker Violet). In addition, the

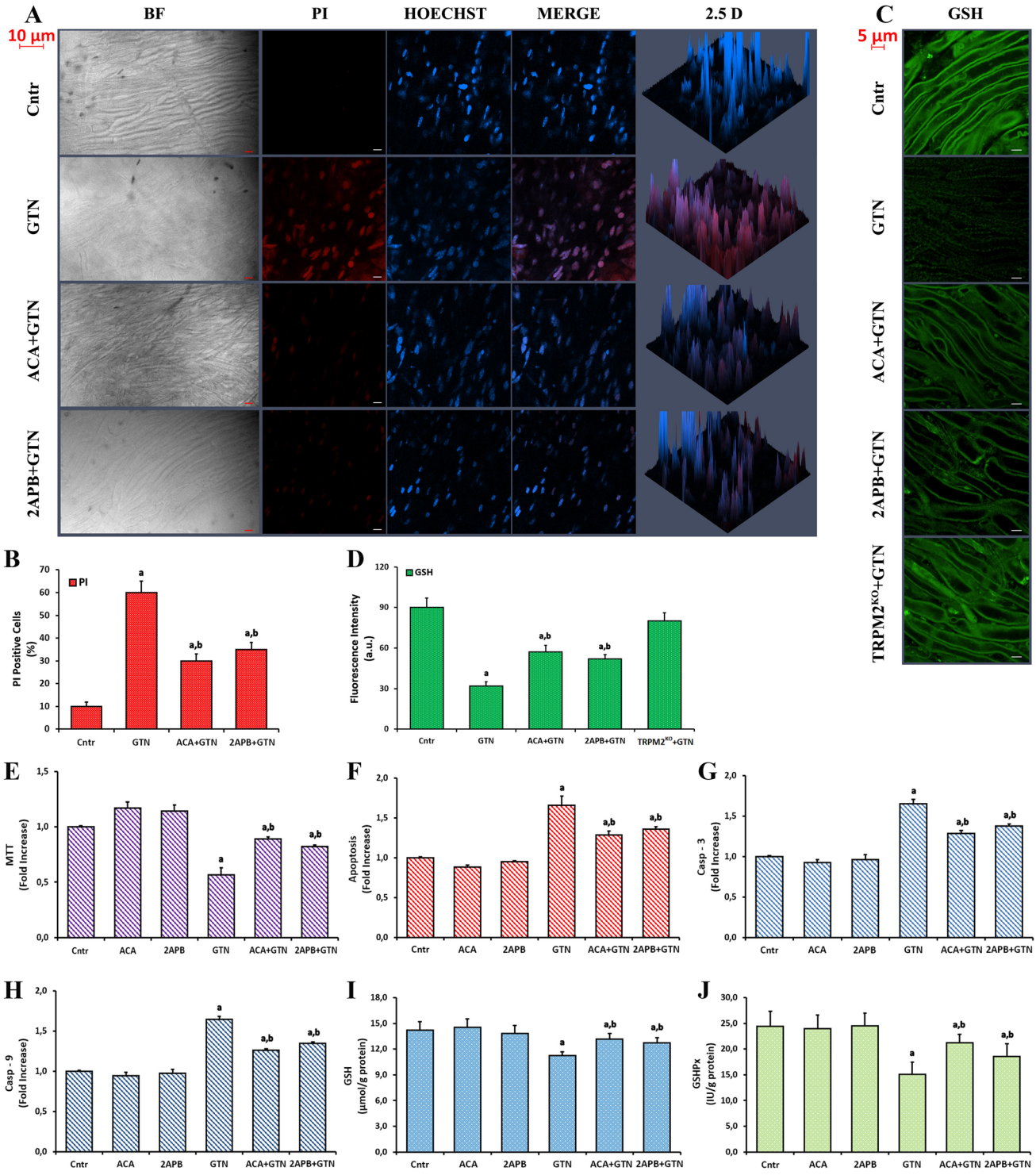

cell viability (MTT), apoptosis, Casp- 3, Casp- 9, GSH, and GSHPx levels were analyzed in the six groups by using the microplate reader and spectrophotometer. In the present study, the rates of TG death (Figs. 3s and b), apoptosis (Fig. 3f), Casp -3 (Fig. 3g), and Casp -9 (Fig. 3h) were higher in the groups of migraine (GTN) than in the groups of non-migraine (Cntr, ACA, and 2APB). However, the increased values were modulated in the group of GTN by the treatments of ACA and 2APB, and their levels were higher in the groups of ACA + GTN and 2APB + GTN than in the group of GTN only ($p \leq 0.05$). The levels of GSH imaging (Figs. 3c and d), cell viability (Fig. 3e), GSH concentration (Fig. 3i), and GSHPx activity (Fig. 3j) were markedly lower in the group of GTN as compared with Cntr ($p \leq 0.05$),

◂**Fig. 3 The treatments of TRPM2 antagonists modulated GTN-mediated the changes of cell death (PI), apoptosis, cell viability, Casp-3, Casp-9, GSH, and GSHPx in the migraine (GTN)-induced trigeminal ganglia of mice.** (Mean ± STD and $n = 10$). The images indicating death (propidium iodide, PI) and live (Hoechst 33,342) (Figs. 3a and b), and GSH concentration (Figs. 3c and d) staining TG neurons of wild-type mice under control conditions or after the treatment of GTN (10 mg/kg), ACA (25 mg/kg), 2APB (5 mg/kg), and their combinations. Each panel consists of bright field (BF), PI (red) and Hoechst (blue)-staining images showing dead and live cells, merge, and 2.5D. Imaging GSH concentration was indicated by green color. The scale bar of BF was kept as 10 μm, although the scale bars of PI/Hoechst and GSH were kept as 5 μm. The cell viability (Fig. 3e) and apoptosis (Fig. 3f) analyses of the TG were performed in the microplate reader using MTT test and commercial kits, respectively. The activity of Casp -3 (Fig. 3g) and Casp -9 (Fig. 3h) were analyzed in the plate reader by using the substrates of the caspase cleavages. The GSH (Fig. 3i), and GSHPx (Fig. 3j) levels were analyzed in the TG by using a spectrophotometer. ($^{a}p \le 0.05$ *vs* Cntr, ACA, TRPM2^{KO}+GTN, and 2APB groups. $^{b}p \le 0.05$ *vs* GTN groups)

although their levels were increased in ACA + GTN and 2APB + GTN by the treatments of ACA and 2APB. However, the changes were not observed in the TGs of TRPM2^{KO} mice, and the values were not decreased or increased in the TGs of TRPM2^{KO} mice by the treatment of GTN. The present results confirmed the involvement of TRPM2 via the decrease of GSH levels on the migraine (GTN)-mediated neuronal toxicity and death in the neurons of TG.

The Migraine (GTN)-Mediated ΔΨm and OS (cROS and mROS) Were Decreased by the Treatment of ACA and 2APB

During the ATP synthesis, ROS was also generated in the mitochondria. Hence, a main source of mROS is mitochondria in body cells by activation of mitochondrial electron transport system [41]. In addition, the increase of mMP (ΔΨm) via the increase of Ca^{2+} influx into cytosol also induces the increase of the mROS generation in several neurons, including the TGs [9, 21, 22]. The increase of ΔΨm and cROS is assayed by using the probes namely JC1 and DCFH-DA/DHR123, respectively. In addition, the increase of the mROS is assayed using the mitochondrial ROS probe (MitoTracker Red CM-H2ros). The generation of ROS is scavenged by the antioxidants, including GSH and GSHPx [10, 11]. In addition, the increase of apoptosis and caspase activation was induced by the increase of mROS generation. After observing the decrease of GSH level and GSHPx activity, but the increase of apoptosis and caspase activation, we suspected whether cROS and mROS production increased through the increase of TRPM2 activation. For this reason, we detected ΔΨm, cROS, and mROS in the migraine-induced TGs of mice by using the stains of JC1, DCFH-DA/DHR123, and MitoTracker Red CM-H2ros.

The levels of ΔΨm (JC1) (Figs. 4a, b, and g), cROS [DCFH-DA (Figs. 4a, c, and h) and DHR123 (Figs. 4d and f)], mROS (Figs. 4d and e), and MDA (Figs. 4i) were increased in the TGs of TRPM2 wild-type mice with the effect of GTN treatment ($p \le 0.05$). However, the treatments of ACA and 2APB diminished the effect of GTN through the inhibition of ΔΨm, cROS, mROS, and MDA in the TG neurons ($p \le 0.05$). The increase in the levels of ΔΨm, cROS, mROS, and MDA following the treatment of GTN corresponded with upregulated the products of cytosolic and mitochondrial OS, although the upregulation of the OS was downregulated in the TGs of TRPM2 wild-type mice by the treatments of TRPM2 antagonist treatments. However, the changes were not observed in the TGs of TRPM2^{KO} mice. Hence, these protective actions of TRPM2 antagonists on the results of ΔΨm, cROS, mROS, and MDA in the TGs further supported the involvement of TRPM2 on mitochondrial OS-induced neuron death.

The GTN-Mediated Increase of Cytosolic Free Ca^{2+} (cCa^{2+}) Fluorescence Intensity in the TRPM2^{WT} TG But Not in the Absence of TRPM2 (TRPM2^{KO}) TG of Mouse

There is a direct relationship between the increase of mitochondrial mROS and the upregulation of TRPA1 and TRPV1-dependent cCa^{2+} concentration in the TGs [3, 8]. The relationship was confirmed in the TRPM2 studies of several neurons, except TGs [18–20, 33]. After observing the increase of mROS via the activation of TRPM2, we suspected the increase of cCa^{2+}concentration via the activation of TRPM2. Fluo-3-AM images of the TRPM2^{WT} TGs in the groups of Cntr and GTN were indicated in the Figs. 5a and b, respectively. The mean florescence intensities of Fluo-3-AM in the Cntr and GTN are shown in the lines (Figs. 5c) and columns (Figs. 5d). In the columns, the concentrations of cCa^{2+} was increased in the TGs by H_2O_2 or CPx stimulations, although they were decreased by the 2APB treatment ($p \le 0.05$). However, the increases of Fluo-3-AM florescence intensities in the groups of TRPM2^{KO} were not observed (Figs. 6a, b, and c) after the stimulation of H_2O_2. The mean florescence intensities of Fluo-3-AM and Fura-2-AM in the Cntr, GTN, ACA + GTN, and 2APB + GTN are shown in the Figs. 5e, f, g, h, and i. The mean florescence intensities of cCa^{2+} concentration were increased in the groups of GTN by the stimulation of H_2O_2 or CPx, although they were decreased by the treatments of TRPM2 antagonists (ACA or 2APB) ($p \le 0.05$).

The enzyme activation of PARP-1 stimulates TRPM2 activation in several neurons such as the hippocampus, DRG, microglia, and sciatic nerve [19, 20, 33]. The DPQ and PJ34 are well-known PARP-1 inhibitors, and they were used in the TRPM2 experiments [33, 42]. Preincubation

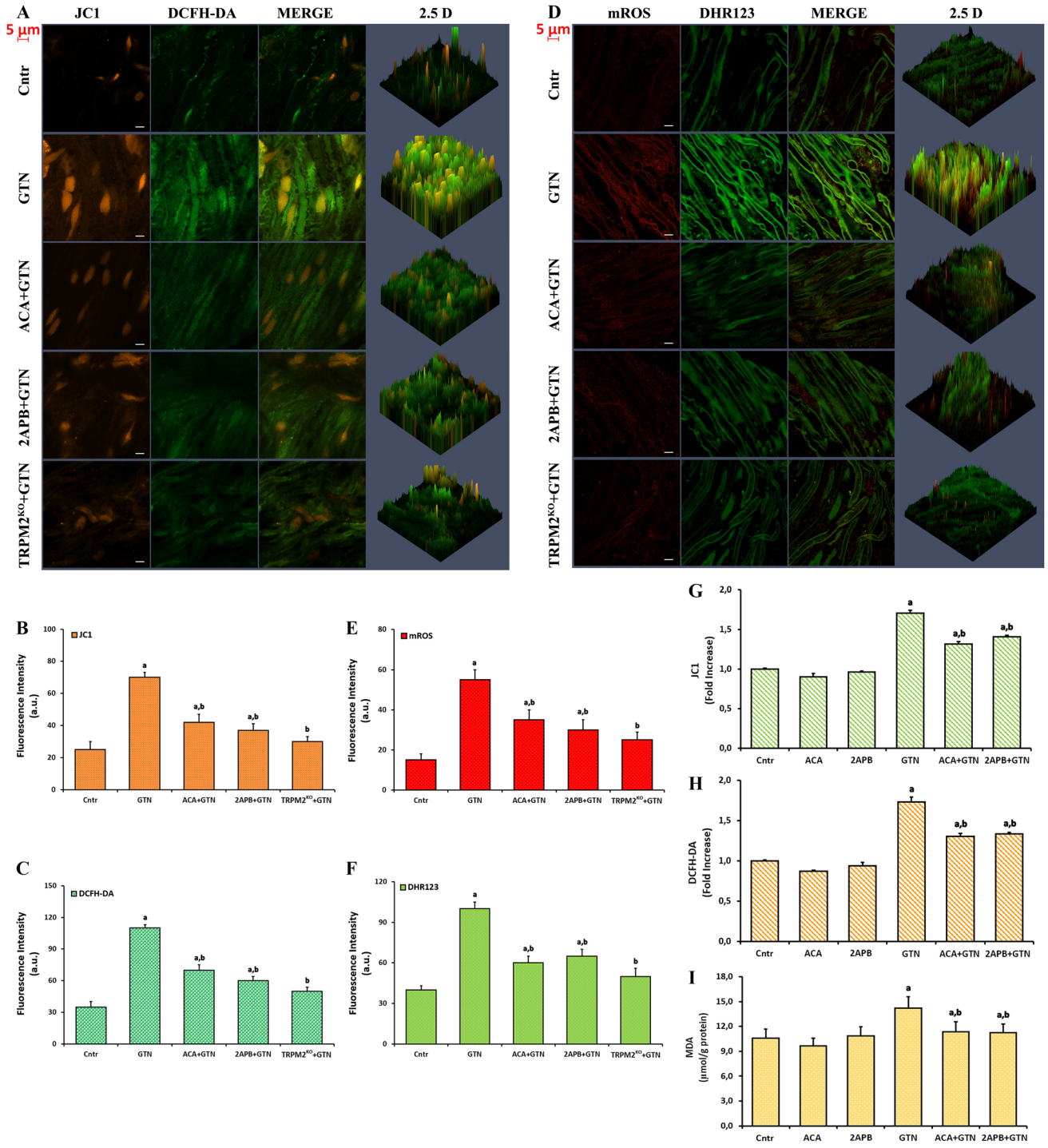

Fig. 4 The experimental migraine (GTN)-induced increase of mitochondrial oxidative stress was decreased by the treatments of TRPM2 antagonists (ACA and 2APB). (Mean ± STD and $n = 10$). The TRPM2 wild-type mice were divided into two main groups as migraine (GTN) and non-migraine. Then, the mice in the both groups received TRPM2 channel blockers (ACA, 25 mg/kg and 2APB, 5 mg/kg) for 3 days. Migraine was induced by a single dose of GTN (10 mg/kg). The effects of GTN (10 mg/kg for 3 days) on the image values in the TGs of TRPM2 knock out mice ($TRPM2^{KO}$). The TG neurons were stained with 2 µM mitochondrial membrane depolarization dye (JC1) (**a** and **b**), cytosolic ROS (cROS) [DCFH-DA (**a** and **c** and **h**) and DHR123 (**d** and **f**)], mitochondrial ROS probe (MitoTracker Red CM-H2ros, Mito-ROS) (**d** and **e**) in the six groups. The TGs were imaged in the CLSM-800 with 40 × oil objective (Scale: 5 µm). The florescence intensity as arbitrary unit (a.u.) was measured by using the ZEN program. The analyses of JC1 (**g**) and DCFH-DA (**h**) were repeated in TGs by using the plate reader (Infinite PRO 200). The levels of lipid peroxidation (MDA) (**i**) were analyzed in the TGs by using the spectrophotometer (Shimadzu-UV1800). ($^{a}p \leq 0.05$ *vs* Cntr, ACA, and 2APB groups. $^{b}p \leq 0.05$ *vs* GTN groups)

of microglia with DPQ and PJ34 acted TRPM2 channel antagonist actions [33], although the action has not been clarified in TGs of mice with migraine. Hence, we want to clarify the effects of the PARP-1 inhibitors on the concentration of cCa^{2+} in the TGs of the GTN group. After PARP-1 enzyme inhibitor pre-incubations of the TGs in the groups of Cntr and GTN, they were activated by the stimulation of H_2O_2, and the images of Fluo-3-AM were captured by using the CLSM-800 (Figs. 6d). We observed that there was no increase of cCa^{2+} concentration in the groups of DPQ + Cntr, PJ34 + Cntr, DPQ + GTN, and PJ34 + GTN after the treatment of H_2O_2 and 2APB (Figs. 6e and 6f).

GTN-Mediated Increase of TRPM2 Current Densities in the TGs Were Diminished by the Treatments of ACA and 2APB

The cell membrane receptor, CD38, has a main role on the activation of TRPM2 via the application of cytosolic ADPR in several neurons [33, 43]. Hence, the TRPM2 channel is activated in neurons such as hippocampus, DRG, and microglia by the application of cytosolic ADPR [19, 20, 33, 36, 38, 39]. However, the activation of TRPM2 via stimulation of cytosolic ADPR has not been reported in the TGs. A best technique for the investigation of cation channels is the patch-clamp technique. After observing the increase of cCa^{2+} concentration, we further wanted to confirm the changes by using the patch-clamp records with whole cell configuration (Fig. 7g). In the absence of the ADPR in the patch pipette (1 mM), there was no current of the TRPM2 in the TGs (Fig. 7a). However, the TRPM2 was gated in the TGs of Cntr group by the cytosolic ADPR (Fig. 7b), and the current density of TRPM2 was higher in the group of Cntr + ADPR (90.97 pA/pF) than in the group of Cntr (4.59 pA/pF) ($p \leq 0.05$) (Fig. 7f). In the GTN group, we observed further the increase of TRPM2 current (Fig. 7c), and the current density was markedly higher in the group of GTN + ADPR (214.85 pA/pF) than in the group of Cntr + ADPR (90.97 pA/pF) (Fig. 7f) ($p \leq 0.05$). However, the current densities in the groups of Cntr + ADPR and GTN + ADPR were upregulated to the control levels by the treatment of ACA (25 μM). The current densities were lower in the groups of Cntr + ADPR + ACA (20.58 pA/pF) and GTN + ADPR + ACA (32.88 pA/pF) than in the groups of Cntr + ADPR and GTN + ADPR ($p \leq 0.05$) (Fig. 7f). However, there was no current in the ACA + GTN + ADPR and 2APB + GTN + ADPR groups after the treatments of ACA (Fig. 7d) and 2APB (Figs. 7e). The current densities were lower in the groups of ACA + GTN + ADPR (6.79 pA/pF) and 2APB + GTN + ADPR (7.39 pA/pF) groups than in the group of GTN + ADPR (214.85 pA/pF) (Fig. 7f).

The Modulator Role of GSH Treatment on GTN-Induced Increase of Pain Intensity and cCa^{2+} Concentration via the Activation of TRPM2 in the TGs of $TRPM2^{WT}$

The decrease of GSH induces TRPM2 activation in the hippocampus, DRG, and microglia, although the treatment of GSH induces a protective action against pain via the inhibition of TRPM2 in rodents [33, 36–40]. However, there is no report of GSH treatment via the inhibition of TRPM2 on the pain intensity and cCa^{2+} in the TGs of rodents and patients with migraine. After observing the decrease of GSH and the increase of pain intensity in the migraine-induced mice, we suspected the protective role of GSH via the inhibition of TRPM2 on the pain intensity and cCa^{2+} in the TGs of migraine-induced mice. The mice received intraperitoneal GSH (200 mg/kg) for 14 days [29]. After 12 h of last GSH administration, migraine was induced by a single dose of GTN (10 mg/kg). In the Cntr, GTN, and GSH + GTN groups, the tests of von Frey (Fig. 8a) and hot plate (Fig. 8b) were performed before GTN treatment and also at 15th day for 1 h with 10-min intervals (total six tests). The mean results of von Frey (Fig. 8c) and hot plate (Fig. 8d) pain intensity test were higher in the group of GTN group as compared with the group of Cntr, although they were lower in the GSH + GTN group than in the GTN group ($p \leq 0.05$). At the end of the GSH treatment experiments, all mice were killed under anesthesia, and the TGs were obtained for staining with Fluo-3-AM. The image of whole TG was captured in the CLSM-800 microscope after the laser stimulation (Fig. 8e). The florescence intensities of cCa^{2+} were measured in the groups of Cntr, GTN, and GSH + GTN by using the ZEN program, and their mean concentrations were indicated by the graphics of column (Fig. 8f). The florescence intensities of cCa^{2+} were higher in the group of GTN group than in the group of Cntr, although they were lower in the group of GSH + GTN as compared with the group of GTN ($p \leq 0.05$). The results are clearly indicated involvement of GSH treatment via the inhibition of TRPM2 on the pain intensity and cCa^{2+} in the TGs of migraine-induced mice.

The GTN-Mediated Activation of TRPM2 Induces Cytokine Responses in the TGs

Recent data indicated that the modulator role of TRPM2 channel blockers on the TRPM2 activation-induced inflammatory responses in the neurons and cell lines [19, 31, 33]. However, there is no report on the modulator role of TRPM2 channel blockers in the GTN-induced cytokine productions in the TGs of TRPM2 wild-type mice. To confirm this, we assayed the concentrations of TNF-α IL-1 β, and IL-6 by

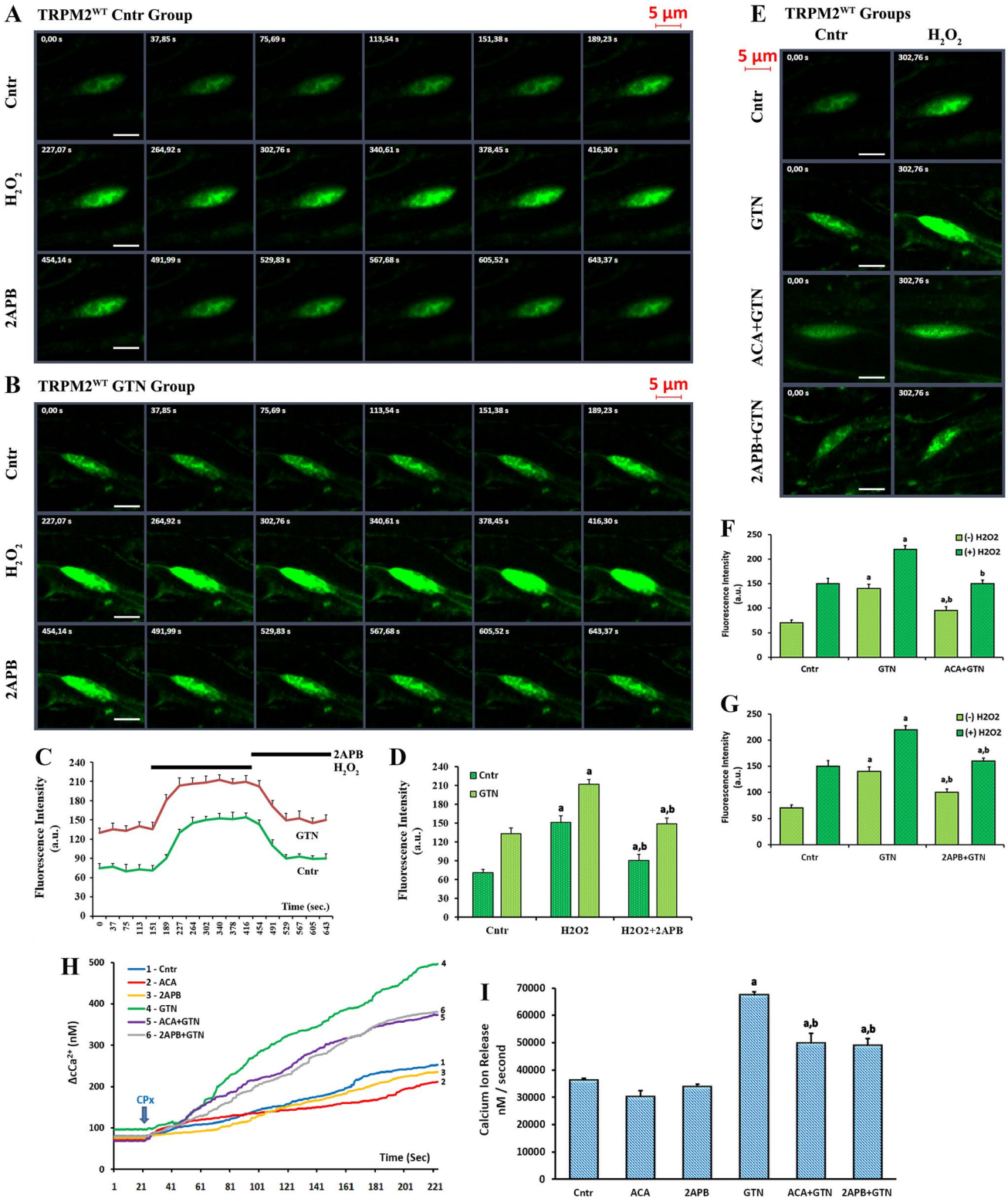

using the commercial ELISA kit. The treatment of mice with GTN upregulated the concentrations of inflammatory cytokines (TNF-α, IL-1β, and IL-6) in the TGs, when compared with control untreated cells (Figs. 9a, b, and c) ($p \leq 0.05$). In contrast, the treatments of TRPM2 channel blockers (ACA and 2APB) again showed downregulations of the TNF-α, IL-1β, and IL-6 concentrations in the TGs after the treatment of GTN ($p \leq 0.05$).

◂**Fig. 5 Migraine (GTN) induces increase of cytosolic free Ca^{2+} (cCa^{2+}) concentration via the activation of TRPM2 in the TG of $TRPM2^{WT}$ mice.** (Mean ± STD and $n = 10$). The TG neurons were divided into six groups as Cntr, ACA, 2APB, GTN, ACA + GTN, and 2APB + GTN. The TG neurons were stained with fluorescent calcium ion indicators namely Fluo-3-AM (1 μM for 45 min) and Fura-2-AM (4 μM for 45 min). The TG neurons were stimulated by TRPM2 against (H_2O_2 or CPx and 1 mM), although they were treated with TRPM2 antagonist (2APB and 100 μM for 10 min) to inhibit Ca^{2+} entry. The image records of Fluo-3-AM in TGs were taken at 515 nm in the CLSM-800 fitted with an objective (×40 oil), although the fluorescent calcium signaling of Fura-2-AM in the TGs was recorded in the Cary Eclipse spectrofluorometer. **a** and **b** Fluo-3-AM imaging and mean Ca^{2+} fluorescence intensity as arbitrary unit (a.u.) in the TGs of Cntr and GTN group, respectively. White numbers in the corner of each image indicate capture time (second). **c** and **d** The mean concentration of Ca^{2+} fluorescence intensity was indicated by the figures of lines and columns, respectively. **e** Fluo-3-AM images in the four groups (Cntr, GTN, ACA + GTN, and 2APB + GTN). **f and g** The mean column graphics of Ca^{2+} fluorescence intensity in the treatments of ACA + GTN and 2APB + GTN, respectively. **h and i** The mean changes in the Ca^{2+} fluorescence intensity (Fura-2-AM) of the TGs in the six groups were indicated by the figures of lines and columns. ($^{a}p \leq 0.05$ *vs* Cntr, ACA, and 2APB groups. $^{b}p \leq 0.05$ *vs* GTN and H_2O_2 groups)

Discussion

We investigated the protective effects of TRPM2 antagonists on Ca^{2+}-induced headache and neurotoxicity, which are two emerging causes for migraine pathogenesis. The neuroprotective effects of TRPM2 channel antagonists against Ca^{2+} influx-induced oxidative cell death were evaluated by using the TG neurons, which have major roles in the etiology of migraine. The findings of the present data show that (1) the TRPM2 channel is involved in the neurobiology of migraine (GTN), TRPM2 activation-mediated pain intensity, $\Delta\Psi m$, cROS, mROS, and neuronal death in the TGs and (2) the treatment of TRPM2 antagonists (ACA and 2APB) attenuated the GTN-induced oxidative injury and Ca^{2+} influx via upregulation of GSH and GSHPx in the TGs of $TRPM2^{WT}$ mice, but not in the TGs of $TRPM2^{KO}$ mice. (3) The protective actions of ACA and 2APB were further increased in the TGs of $TRPM2^{WT}$ mice by PARP1 (PJ34 and DPQ) inhibitors. (4) The treatment of GSH via inhibition of TRPM2 was also diminished the GTN-induced pain intensity and cCa^{2+} concentration in the TGs of TGs of $TRPM2^{WT}$ mice (Fig. 10). Collectively, this suggests the involvement of GTN-induced oxidative cytotoxicity and TRPM2 via excessive Ca^{2+} influx to the TGs in the etiology of migraine.

A member of the Ca^{2+} permeable TRP superfamily is the TRPM2 cation channel, and it is activated by ADPR and OS [15, 16]. TRPM2 plays an important role on neuronal life and differentiation [44]. The generations of cROS and mROS are required in body cells by performing several physiological functions such as killing bacteria and viruses. However, a high concentration of OS leads to loss of neuronal physiology and is involved in the pathogenesis of oxidative pain and headache disorders, including migraine [45, 46]. Two common pathways of oxidative neurotoxicity have been described. One is the OS redox pathway, which is mediated by the TRPM2 action-mediated excessive Ca^{2+} influx. The mechanism of neurotoxicity has been extensively clarified, and it is believed that transient increases of cCa^{2+} influxes lead to accumulation into mitochondria, increases in the levels of cROS and mROS, and ultimately apoptosis and cell death via the activations of Casp -3 and Casp -9 [13, 19, 20, 31, 47, 48]. In the current data, we observed the GTN-mediated increase of pain intensity, cCa^{2+}, cROS, and mROS via the increase of TRPM2 current density in the TGs of mice. In accordance with the present results, the involvements of TRPM2 in the pain diseases such as fibromyalgia and neuropathic pain were recently reported [13, 19]. The second different pathway in the cROS and mROS-mediated neurotoxicity involves oxidation of cysteine redox system, which is required for the TRPM2 activation [33, 49]. The decrease of members in the cysteine redox system such as GSH and selenium by high concentrations of cROS and mROS leads to an imbalance in neuronal cysteine homeostasis, a reduction in neuronal GSH concentrations, and the increase of mROS generation [50]. The decrease of plasma GSH concentration in the rodents and patients with headache and migraine was deeply reported [10, 11, 45, 46]. The GSH depletion-induced TRPM2 activation caused to the increase of oxidative neurotoxicity in the neuronal SH-SY5Y cell line, primary neuronal cultures, and microglia in the several disease models, except the migraine (GTN) model [33, 36–40]. In the present data, we observed the increase of GTN-mediated overload cCa^{2+} via the activation of TRPM2 and the overload cCa^{2+} caused to the decrease of GSH concentration and GSHPx activity in the TGs. However, the inhibition of GTN-induced overload cCa^{2+} via the modulation of TRPM2 increased GSH concentration and GSHPx activity in the TGs. The results clearly indicated the importance of the thiol redox system and GSH concentration on the TRPM2 activation in the migraine etiology.

Accumulating evidence supports that TRPM2-mediated Ca^{2+} signaling pathways are associated with mROS in the TG neurons [17]. We confirmed that the treatments of TRPM2 blockers (ACA and 2APB) and antioxidant (GSH) fully reversed the TRPM2-induced cell death. Yıldızhan and Nazıroğlu [33] reported that the treatments of GSH and TRPM2 blockers restored overload cCa^{2+}-induced neuronal death in the microglia culture of mice. These imply that OS and TRPM2-mediated Ca^{2+} dysregulation are the crucial that orchestrate the subsequent neurotoxicity pathologic pathways involved in the TRPM2-mediated toxicity in the migraine (GTN) mice model. To examine the protective actions of TRPM2 antagonists on the TRPM2-induced cROS and mROS generations were assayed using DCFH-DA,

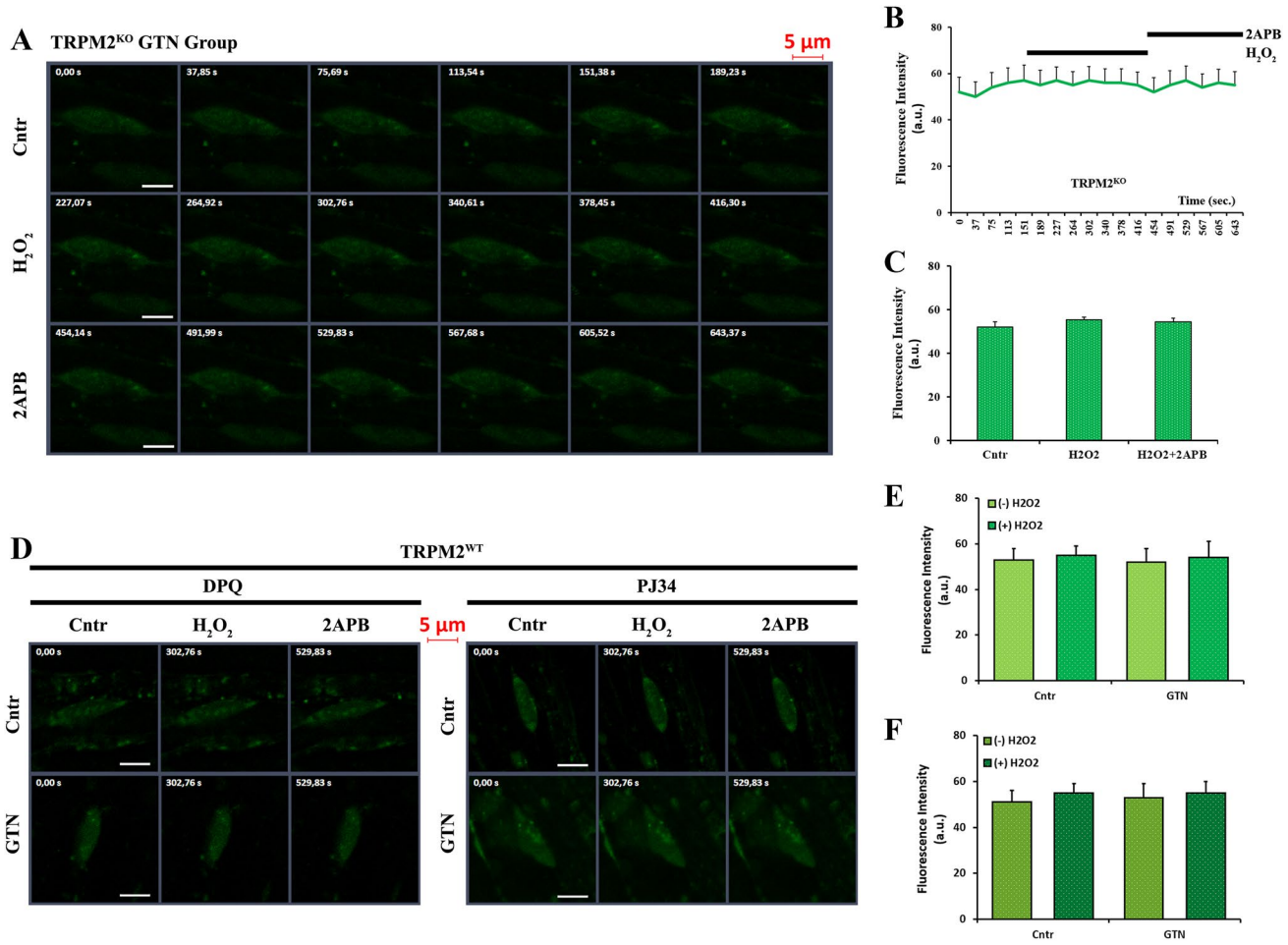

Fig. 6 There were no GTN treatment-induced increases of cytosolic free Ca^{2+} concentrations in the TGs of $TRPM2^{KO}$ mice and $TRPM2^{WT}$ mice pretreated with PARP-1 and TRPM2 inhibitors. (Mean ± STD and $n = 10$). **a** The TGs of $TRPM2^{KO}$ in the GTN group were stained with Fluo-3-AM (1 μM for 60 min). The TG neurons were stimulated by H_2O_2 (1 mM for 3–4 min), but they were inhibited by 2APB (100 μM for 3–4 min) after loading Fluo-3-AM. The samples were analyzed in the CLSM-800. **b and c** Fluorescence intensity changes of Ca^{2+} in the TGs of $TRPM2^{KO}$ mice were indicated by line and column. The TGs of $TRPM2^{WT}$ in the control and GTN were pretreated with PARP-1 inhibitors (30 nM DPQ for 30 min and 1 μM PJ34 for 30 min) before stimulation of H_2O_2 (1 mM). **d** The imagines of Ca^{2+} in the Cntr and GTN groups of $TRPM2^{WT}$ mice after DPQ and PJ34 treatments. **e and f** The mean fluorescence intensity changes of Ca^{2+} in the Cntr and GTN groups of $TRPM2^{WT}$ mice after DPQ and PJ34 treatments

DHR123, and MitoTracker Red CM-H2ros staining followed by CLSM-800 analysis. The GTN-mediated activation of TRPM2 significantly increased cROS and mROS, suggesting that the activation of TRPM2 increased the generations of cytosolic and mitochondrial ROS in TG neurons of GTN-treated mice. However, co-treatment of TRPM2 antagonists reversed GTN-induced cROS and mROS productions in the groups of ACA + GTN and 2APB + GTN. These data indicate that the activity of TRPM2 for homeostatic control of cCa^{2+} and mROS levels may underlie the protective actions against GTN-induce neurotoxicity.

The DNA damage-induced ADPR in the nucleus of neurons is produced by the activation of PARP-1 and responds when ADPR binds to the channel's enzymatic nudix C domain [50, 51]. The activity of TRPM2 is inhibited by the treatments of ACA and 2APB [52, 53]. The OS-mediated apoptosis and death in the TGs were induced by the excessive Ca^{2+} influx [3, 25]. The involvement of glutamate-mediated Ca^{2+} influx was investigated on the apoptosis and death in the TG neurons [54]. The excessive OS generation and overload Ca^{2+} influx are two main factors on the inductions of headache and pain in the human and rodents [10, 11]. Two members of the TRP superfamily are TRPA1 and TRPV1 channels, and they are also activated by OS [8, 13]. The involvements of TRPA1 and TRPV1 on the GTN-mediated migraine and pain models were recently reported [55–57]. Within the OS-dependent-activated TRP channels, TRPM2 is first discovered channel [15, 16]. Because of the involvement of OS and Ca^{2+} influx in the etiology of migraine, TRPM2 is a potent channel for the induction of

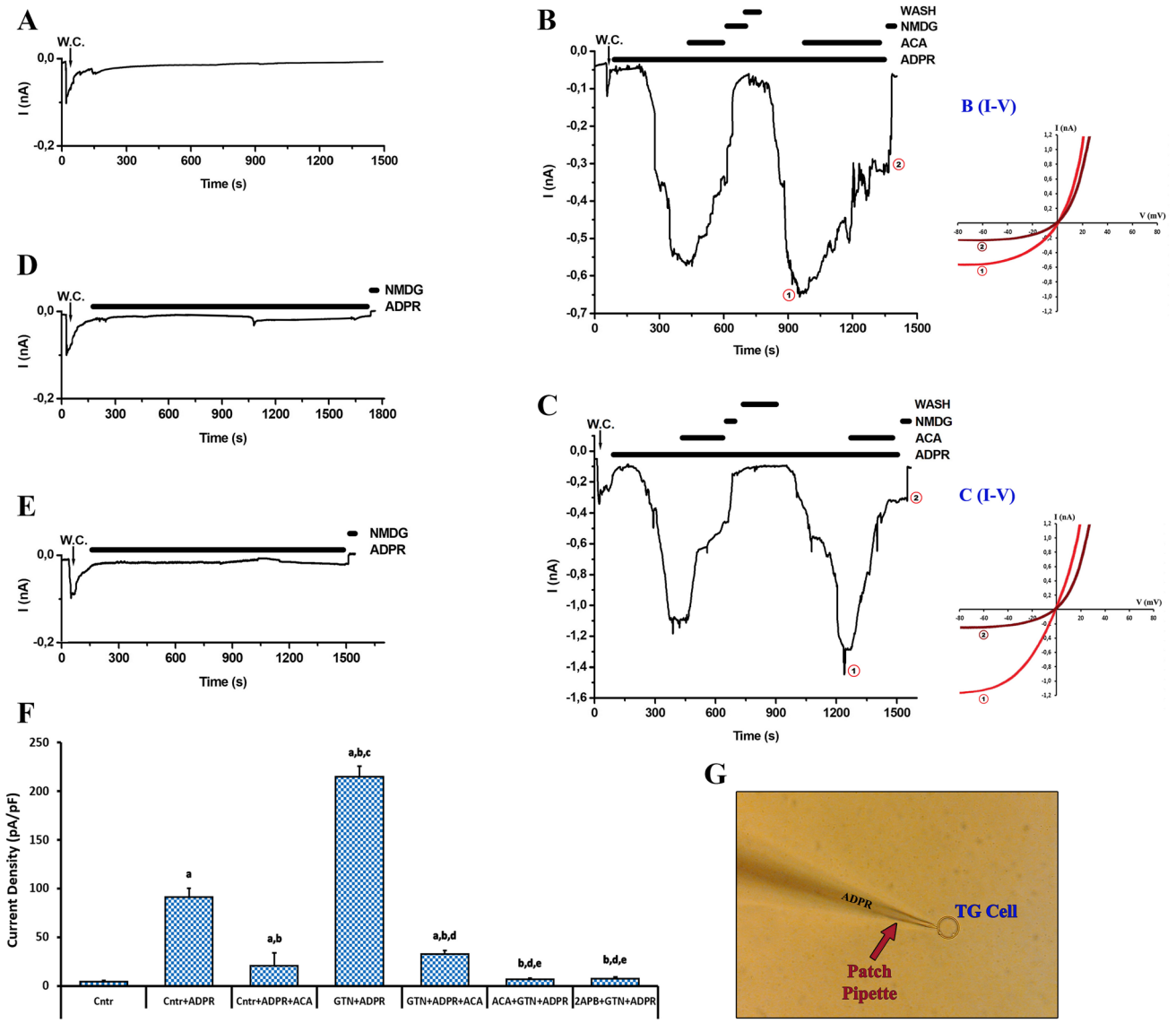

Fig. 7 The GTN induced increase of TRPM2 current densities in the TGs. ($n=3$ and mean ± STD). W.C.: whole cell patch-clamp configuration. **a** Control (Cntr) (without ADPR stimulation). **b** Cntr + ADPR with the treatment of ADPR and ACA. **c** GTN + ADPR group with the treatments of ADPR and ACA after the treatment of GTN. **d** ACA + GTN + ADPR group with the treatment of ADPR after the treatments of ACA (25 mg/kg/day for 3 days) and GTN (10 mg/kg/day for one day). **e** 2APB + GTN + ADPR group with the treatment of ADPR after the treatments of 2APB (5 mg/kg/day for 3 days) and GTN (10 mg/kg/day for one day). **f** The mean current densities of TRPM2. **g** Picture of whole cell configuration of the TGs under microscope. ($^{a}p \leq 0.05$ vs Cntr. $^{b}p \leq 0.05$ vs Cntr + ADPR group. $^{c}p \leq 0.05$ vs Cntr + ADPR + ACA group. $^{d}p \leq 0.05$ vs GTN + ADPR group. $^{e}p \leq 0.05$ vs GTN + ADPR + ACA group)

migraine. Hence, we investigated the protective actions of TRPM2 channel blockers and PARP-1 inhibitors on the Ca^{2+} influx in the TG neurons of $TRPM2^{WT}$ and $TRPM2^{KO}$ mice. The results of the Fluo-3-AM and Fura-2-AM indicated an increase of cCa^{2+} concentration via the activation TRPM2 in the TGs of GTN-treated $TRPM2^{WT}$ mice, but not in the TGs of $TRPM2^{KO}$ mice and $TRPM2^{WT}$ mice treated with PARP-1 inhibitors (DPQ and PJ34). However, the H_2O_2 and ADPR-mediated increases of cCa^{2+} concentration were diminished by the treatments of TRPM2 antagonists and PARP-1 inhibitors. Hence, the data of PARP-1 inhibitor and TRPM2 antagonists confirmed the involvement of TRPM2 on the increase of cCa^{2+} concentration in the TGs of GTN treated mice.

The generations of cytokines such as TNF-α, IL-1β, and IL-6 induce important roles in the activation of nerve terminals for the induction neuro-inflammation. The increase of pro-inflammatory cytokine concentrations, including the concentrations of TNF-α, IL-1β, and IL-6, was recently reported in migraine patients [58]. The increase of TNF-α,

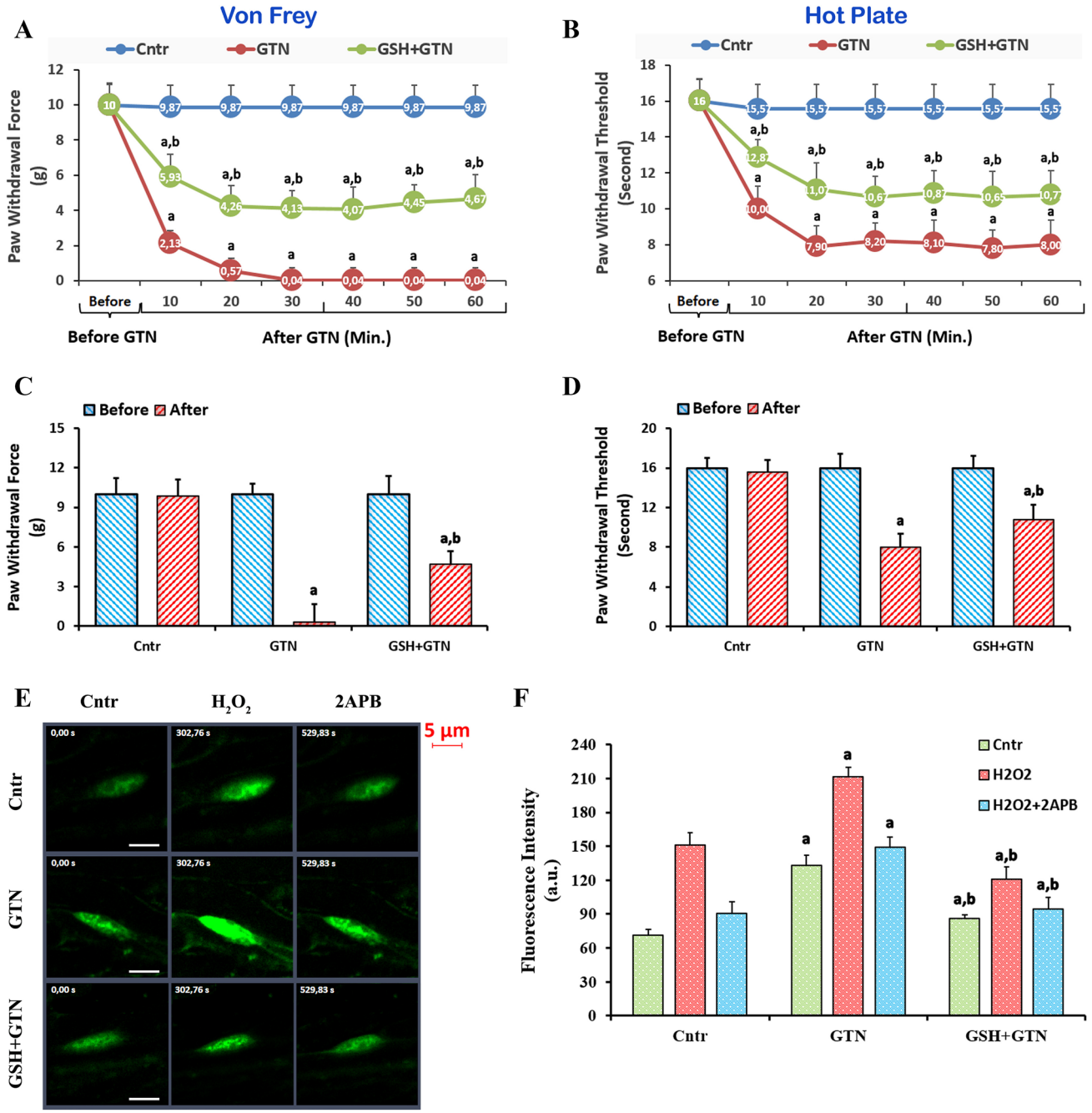

Fig. 8 The GTN induced increases of pain intensity and cytosolic free Ca^{2+} concentration in the TGs were decreased by the treatment of GSH. ($n = 3$ and mean ± STD). The mice received 14 days intraperitoneal GSH (200 mg/kg). After 12 h of last dose administration, migraine was induced by a single dose of GTN (10 mg/kg). In the Cntr, GTN, and GSH + GTN groups, the hyperalgesia tests of von Frey (**a**) and hot plate (**b**) were performed at basal level, and also at 15th day for 1 h with 10-min interval (total six tests). The mean values of von Frey (**c**) and hot plate (**d**) were shown by lines. At the end of the experiments, all mice were decapitated under anesthesia, and the whole trigeminal ganglia (TG) was obtained for staining with 1 µM Fluo-3-AM for 60 min. **e** The images of whole TG were captured in the CLSM-800 microscope after the laser stimulation. The florescence intensities of cCa^{2+} were measured in the groups of Cntr, GTN, and GSH + GTN by using the ZEN program, and their mean concentrations were indicated by the graphics of line (**f**) and column (**g**). ($^{a}p \leq 0.05$ *vs* Cntr group. $^{b}p \leq 0.05$ *vs* GTN group)

IL-1β, and IL-6 concentrations via the activation of voltage gated calcium channels and glutamate systems in the TGs of mice with migraine was also reported [59, 60]. Recent data indicated that the modulator role of TRPM2 channel blockers on the TRPM2 activation-induced inflammatory responses in the neurons and cell lines [19, 31, 33, 61]. To

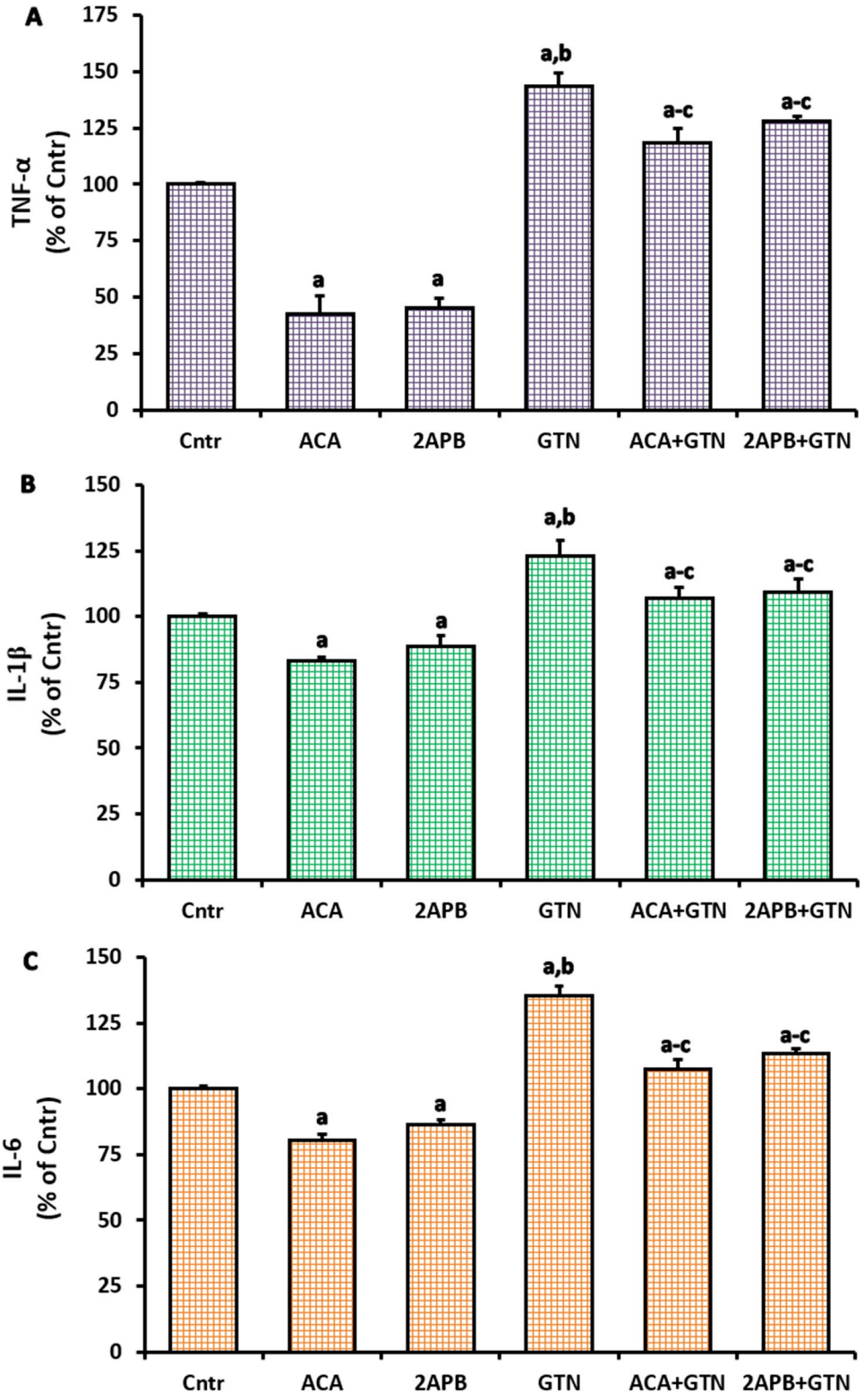

Fig. 9 The GTN-induced increases of cytokine concentrations were diminished in TGs by the treatments of TRPM2 channel antagonists. (Mean ± SD and $n = 6$). The concentrations of TNF-α (**a**), IL-1β (**b**), and IL-6 (**c**) were measured in the ELISA by using the commercial mice kits. ([a]$p \leq 0.05$ *vs* Cntr group. [b]$p \leq 0.05$ *vs* ACA, and 2APB groups. [c]$p \leq 0.05$ *vs* GTN group)

our knowledge, there is no report on the cytokine generation and TRPM2 activation in the TGs of mice with migraine. In the current study, the treatment of mice with GTN increased the concentrations of TNF-α, IL-1β, and IL-6 in the TGs, when compared with control untreated cells. In contrast, the treatments of ACA and 2APB again indicated a decrease of the TNF-α, IL-1β, and IL-6 concentrations in the TGs after the treatment of GTN.

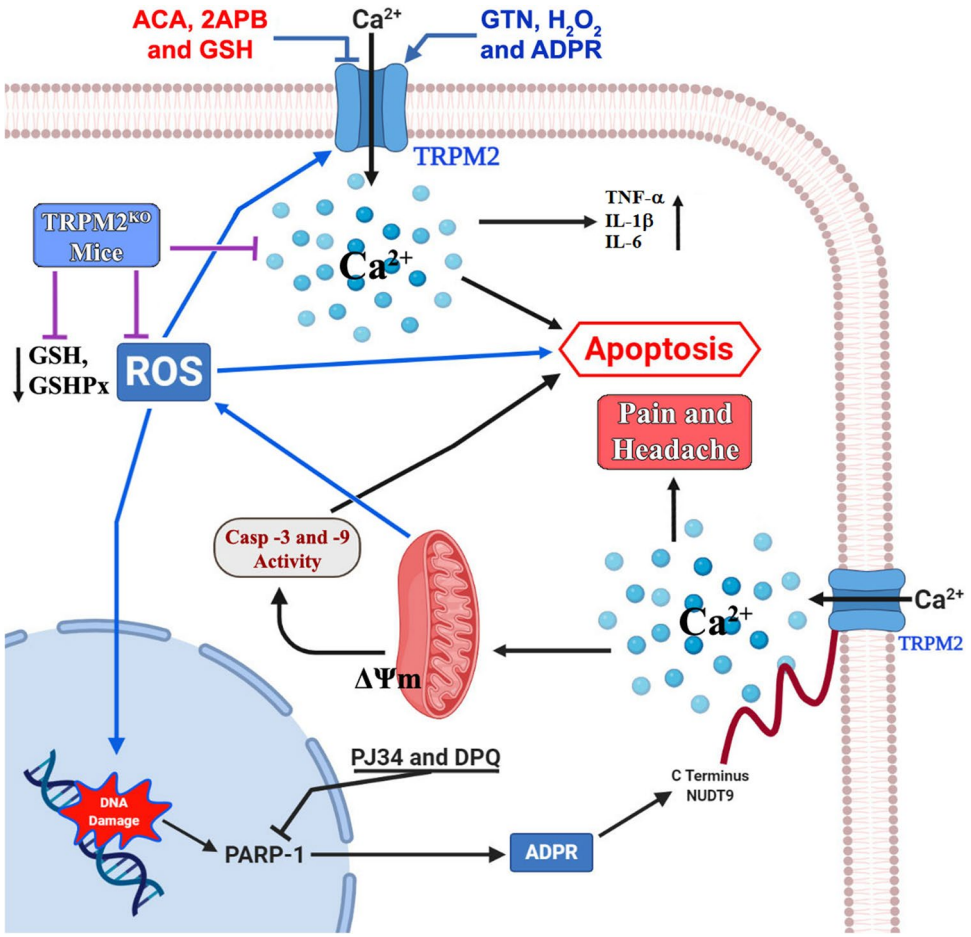

Fig. 10 The possible protective action of GSH and TRPM2 antagonists on the molecular pathways of oxidative stress, apoptosis, and pain intensity in the trigeminal ganglia (TG) of mice with migraine (GTN). Accumulating evidences indicate that the generations of H_2O_2 and DNA-damage (via the activation of PARP-1)-induced ADP-ribose (ADPR) stimulate TRPM2, although the treatments of glutathione (GSH), ACA, and 2APB inhibit the activity of TRPM2. The increase of cytosolic free Ca^{2+} (cCa^{2+}) via the activation of TRPM2 in the cytosol of TGs causes the increase of mitochondrial membrane depolarization (ΔΨm). In turn, the increase of ΔΨm causes the excessive generations of cytosolic (cROS), mitochondrial (mROS) oxidative stress, cytokines (TNF-α, IL1β, and IL-6), and the decrease of cytosolic GSH and glutathione peroxidase (GSHPx) level. However, the effects of GTN were not observed in the TG of TRPM2 knockout ($TRPM2^{KO}$) mice. The GTN and TRPM2 activation-mediated excessive Ca^{2+} influx cause apoptosis and cell death via the activations of caspase pathways such as caspase-3 and caspase-9 in the TGs. The pain, oxidant, and apoptotic actions of GTN are modulated by the treatments of TRPM2 antagonists (GSH, ACA, and 2APB) and PARP-1 inhibitors (PJ34 and DPQ). (↑) Increase. (↓) Decrease

In conclusions, the GTN-induced activation of TRPM2 increased the levels of pain intensity, cROS, mROS, cCa^{2+}, cytokine, and ΔΨm, suggesting that TRPM2-induced neurotoxicity and pain are medicated by the upregulation of OS and inflammation, Ca^{2+} dysregulation, and irreversible mitochondrial dysfunction, and downregulation of GSH and GSHPx. The treatment of TRPM2 antagonists (ACA and 2APB), PARP-1 inhibitors (DPQ and PJ34), and GSH inhibited all of these TRPM2-mediated cytotoxic events and sustained TG neuronal survival from the TRPM2-induced apoptosis and death. Our findings support that the treatments of TRPM2 antagonists and GSH are responsible for the neuroprotective effects of TRPM2 inhibition. Therefore, the modulation of TRPM2 via its antagonists and GSH treatment in the TGs of experimental migraine model can be discovered for new drug targets to control migraine-induced headache and oxidative neurotoxicity.

Acknowledgements The study was summarized from PhD Thesis of Y. Yazğan (Supervisor: Professor M. Nazıroğlu).

Authors' Contribution Dr. Nazıroğlu reviewed the current literature, and designed the project. Mr. Y Yazğan performed animal care, patch clamp, and spectrofluorometer tests. Dr. Nazıroğlu conceptualized this perspective piece, reviewed and revised the manuscript.

Funding This study was supported by the Scientific Research Project Unit (BAP), Suleyman Demirel University, Isparta, Turkey (Project No: TDK-2020–7448: Project Owner: M. Nazıroğlu).

Data availability The treatments and animal tissue samplings in the current study were induced in BMAU. The present analyses were performed in BSN Health, Analyses, Innovation, Consultancy, Organization, Agriculture, and Industry Ltd, (Göller Bölgesi Teknokenti, Isparta, Turkey) and they are available from the M. Nazıroğlu on reasonable request. All graphics including graphical abstract in the manuscript were prepared by a co-author (PhD Student Y. Yazğan).

Declarations

Ethics approval This article does not contain any studies with human participants performed by any of the authors. The present study was performed with the approval of the Experimental Animal Ethics Committee of Burdur Mehmet Akif University (Number: 2019–602. Date: 18.12.2019). The authors have no ethical conflicts to disclose.

Consent to participate Dr. Nazıroğlu reviewed the current literature, and designed the project. Mr. Y Yazğan performed animal care, patch clamp, and spectrofluorometer tests. Dr. Nazıroğlu conceptualized this perspective piece, reviewed and revised the manuscript. All authors approved the final manuscript as submitted.

Consent for publication All authors approved the final manuscript as submitted.

Conflict of Interest The authors have no conflicts of interest to declare.

References

1. Ashina M, Katsarava Z, Do TP, Buse DC, Pozo-Rosich P, Özge A et al (2021) Migraine: epidemiology and systems of care. Lancet 397(10283):1485–1495. https://doi.org/10.1016/S0140-6736(20)32160-7
2. Yeh WZ, Blizzard L, Taylor BV (2018) What is the actual prevalence of migraine? Brain Behav 8(6):e00950. https://doi.org/10.1002/brb3.950
3. Abushik PA, Niittykoski M, Giniatullina R, Shakirzyanova A, Bart G, Fayuk D, Sibarov DA, Antonov SM et al (2014) The role of NMDA and mGluR5 receptors in calcium mobilization and neurotoxicity of homocysteine in trigeminal and cortical neurons and glial cells. J Neurochem 129(2):264–274. https://doi.org/10.1111/jnc.12615
4. Shatillo A, Koroleva K, Giniatullina R, Naumenko N, Slastnikova AA, Aliev RR, Bart G, Atalay M et al (2013) Cortical spreading depression induces oxidative stress in the trigeminal nociceptive system. Neuroscience 253:341–349. https://doi.org/10.1016/j.neuroscience.2013.09.002
5. Park HJ, Kwak M, Baek SH (2020) Neuroprotective effects of Dendropanax morbifera leaves on glutamate-induced oxidative cell death in HT22 mouse hippocampal neuronal cells. J Ethnopharmacol 251:112518. https://doi.org/10.1016/j.jep.2019.112518
6. Dong X, Guan X, Chen K, Jin S, Wang C, Yan L, Shi Z, Zhang X et al (2017) Abnormal mitochondrial dynamics and impaired mitochondrial biogenesis in trigeminal ganglion neurons in a rat model of migraine. Neurosci Lett 636:127–133. https://doi.org/10.1016/j.neulet.2016.10.054
7. Li X, Jiang LH (2019) A critical role of the transient receptor potential melastatin 2 channel in a positive feedback mechanism for reactive oxygen species-induced delayed cell death. J Cell Physiol 234(4):3647–3660. https://doi.org/10.1002/jcp.27134
8. Marone IM, De Logu F, Nassini R, De Carvalho GM, Benemei S, Ferreira J, Jain P et al (2018) TRPA1/NOX in the soma of trigeminal ganglion neurons mediates migraine-related pain of glyceryl trinitrate in mice. Brain 141(8):2312–2328. https://doi.org/10.1093/brain/awy177
9. Borkum JM (2016) Migraine triggers and oxidative stress: A narrative review and synthesis. Headache 56(1):12–35. https://doi.org/10.1111/head.12725
10. Nazıroğlu M, Çelik Ö, Uğuz AC, Bütün A (2015) Protective effects of riboflavin and selenium on brain microsomal Ca2+-ATPase and oxidative damage caused by glyceryl trinitrate in a rat headache model. Biol Trace Elem Res 164(1):72–79. https://doi.org/10.1007/s12011-014-0199-x
11. Bütün A, Nazıroğlu M, Demirci S, Çelik Ö, Uğuz AC (2015) Riboflavin and vitamin E increase brain calcium and antioxidants, and microsomal calcium-ATP-ase values in rat headache models induced by glyceryl trinitrate. J Membr Biol 248(2):205–213. https://doi.org/10.1007/s00232-014-9758-5
12. Ishii M, Iizuka R, Kiuchi Y, Mori Y, Shimizu S (2011) Neuroprotection by lomerizine, a prophylactic drug for migraine, against hydrogen peroxide-induced hippocampal neurotoxicity. Mol Cell Biochem 358(1 2):1–11. https://doi.org/10.1007/s11010-011-0913-3
13. Carrasco C, Naziroğlu M, Rodríguez AB, Pariente JA (2018) Neuropathic pain: Delving into the oxidative origin and the possible implication of transient receptor potential channels. Front Physiol 9:95. https://doi.org/10.3389/fphys.2018.00095
14. Shibata M, Tang C (2021) Implications of transient receptor potential cation channels in migraine pathophysiology. Neurosci Bull 37(1):103–116. https://doi.org/10.1007/s12264-020-00569-5
15. Hara Y, Wakamori M, Ishii M, Maeno E, Nishida M, Yoshida T et al (2002) LTRPC2 Ca2+-permeable channel activated by changes in redox status confers susceptibility to cell death. Mol Cell 9(1):163–173. https://doi.org/10.1016/S1097-2765(01)00438-5
16. Nazıroğlu M, Lückhoff A (2008) Effects of antioxidants on calcium influx through TRPM2 channels in transfected cells activated by hydrogen peroxide. J Neurol Sci 270(1–2):152–158. https://doi.org/10.1016/j.jns.2008.03.003
17. Chung MK, Asgar J, Lee J, Shim MS, Dumler C, Ro JY (2015) The role of TRPM2 in hydrogen peroxide-induced expression of inflammatory cytokine and chemokine in rat trigeminal ganglia. Neuroscience 297:160–169. https://doi.org/10.1016/j.neuroscience.2015.03.067
18. Nazıroğlu M, Özgül C, Çelik Ö, Çiğ B, Sözbir E (2011) Aminoethoxydiphenyl borate and flufenamic acid inhibit Ca2+ influx through TRPM2 channels in rat dorsal root ganglion neurons activated by ADP-ribose and rotenone. J Membr Biol 241(2):69–75. https://doi.org/10.1007/s00232-011-9363-9
19. Yüksel E, Nazıroğlu M, Şahin M, Çiğ B (2017) Involvement of TRPM2 and TRPV1 channels on hyperalgesia, apoptosis and oxidative stress in rat fibromyalgia model: Protective role of selenium. Sci Rep 7(1):17543. https://doi.org/10.1038/s41598-017-17715-1
20. Uslusoy F, Nazıroğlu M, Çiğ B (2017) Inhibition of the TRPM2 and TRPV1 channels through *Hypericum perforatum* in sciatic nerve injury-induced rats demonstrates their key role in apoptosis and mitochondrial oxidative stress of sciatic nerve and dorsal Root ganglion. Front Physiol 8:335. https://doi.org/10.3389/fphys.2017.00335
21. Koroleva K, Mustafina A, Yakovlev A, Hermann A, Giniatullin R, Sitdikova G (2017) Receptor mechanisms mediating the pronociceptive action of hydrogen sulfide in rat trigeminal neurons

and meningeal afferents. Front Cell Neurosci 11:226. https://doi.org/10.3389/fncel.2017.00226
22. Rusu MC, Mănoiu VS, Vrapciu AD, Hostiuc S, Mirancea N (2016) Altered mitochondrial anatomy of trigeminal ganglia neurons in diabetes. Anat Rec (Hoboken) 299(11):1561–1570. https://doi.org/10.1002/ar.23475
23. Bawa B, Abbott LC (2008) Analysis of calcium ion homeostasis and mitochondrial function in cerebellar granule cells of adult CaV 2.1 calcium ion channel mutant mice. Neurotox Res 13(1):1–18. https://doi.org/10.1007/BF03033363
24. Gover TD, Moreira TH, Kao JP, Weinreich D (2007) Calcium homeostasis in trigeminal ganglion cell bodies. Cell Calcium 41(4):389–396. https://doi.org/10.1016/j.ceca.2006.08.014
25. Pecze L, Jósvay K, Blum W, Petrovics G, Vizler C, Oláh Z, Schwaller B (1863) (2016) Activation of endogenous TRPV1 fails to induce overstimulation-based cytotoxicity in breast and prostate cancer cells but not in pain-sensing neurons. Biochim Biophys Acta 8:2054–2064. https://doi.org/10.1016/j.bbamcr.2016.05.007
26. Gross EC, Putananickal N, Orsini AL, Vogt DR, Sandor PS, Schoenen J, Fischer D (2021) Mitochondrial function and oxidative stress markers in higher-frequency episodic migraine. Sci Rep 11(1):4543. https://doi.org/10.1038/s41598-021-84102-2
27. Çakır M, Tekin S, Taşlıdere A, Çakan P, Düzova H, Gül CC (2019) Protective effect of N-(p-amylcinnamoyl) anthranilic acid, phospholipase A_2 enzyme inhibitor, and transient receptor potential melastatin-2 channel blocker against renal ischemia-reperfusion injury. J Cell Biochem 120(3):3822–3832. https://doi.org/10.1002/jcb.27664
28. Wacker MJ, Kosloski LM, Gilbert WJ, Touchberry CD, Moore DS, Kelly JK, Brotto M, Orr JA (2009) Inhibition of thromboxane A2-induced arrhythmias and intracellular calcium changes in cardiac myocytes by blockade of the inositol trisphosphate pathway. J Pharmacol Exp Ther 331(3):917–924. https://doi.org/10.1124/jpet.109.157677
29. Hamers FP, Brakkee JH, Cavalletti E, Tedeschi M, Marmonti L, Pezzoni G, Neijt JP, Gispen WH (1993) Reduced glutathione protects against cisplatin-induced neurotoxicity in rats. Cancer Res 53(3):544–549
30. Abuarab N, Munsey TS, Jiang LH, Li J, Sivaprasadarao A (2017) High glucose-induced ROS activates TRPM2 to trigger lysosomal membrane permeabilization and Zn^{2+}-mediated mitochondrial fission. Sci Signal 10(490):eaal4161. https://doi.org/10.1126/scisignal.aal4161
31. Nazıroğlu M, Çiğ B, Yazğan Y, Schwaerzer GK, Theilig F, Pecze L (2019) Albumin evokes Ca^{2+}-induced cell oxidative stress and apoptosis through TRPM2 channel in renal collecting duct cells reduced by curcumin. Sci Rep 9(1):12403. https://doi.org/10.1038/s41598-019-48716-x
32. Ertilav K (2019) Pregabalin protected cisplatin-induced oxidative neurotoxicity in neuronal cell line. J Cell Neurosci Oxid Stress 11(1):815–824
33. Yıldızhan K, Nazıroğlu M (2020) Glutathione depletion and parkinsonian neurotoxin MPP^+-induced TRPM2 channel activation play central roles in oxidative cytotoxicity and inflammation in microglia. Mol Neurobiol 57(8):3508–3525. https://doi.org/10.1007/s12035-020-01974-7
34. Joshi DC, Bakowska JC (2011) Determination of mitochondrial membrane potential and reactive oxygen species in live rat cortical neurons. J Vis Exp 23(51):2704. https://doi.org/10.3791/2704
35. Keil VC, Funke F, Zeug A, Schild D, Müller M (2011) Ratiometric high-resolution imaging of JC-1 fluorescence reveals the subcellular heterogeneity of astrocytic mitochondria. Pflugers Arch 462:693–708. https://doi.org/10.1007/s00424-011-1012-8
36. Övey IS, Nazıroğlu M (2015) Homocysteine and cytosolic GSH depletion induce apoptosis and oxidative toxicity through cytosolic calcium overload in the hippocampus of aged mice: involvement of TRPM2 and TRPV1 channels. Neuroscience 284:225–233. https://doi.org/10.1016/j.neuroscience.2014.09.078
37. Belrose JC, Xie YF, Gierszewski LJ, MacDonald JF, Jackson MF (2012) Loss of glutathione homeostasis associated with neuronal senescence facilitates TRPM2 channel activation in cultured hippocampal pyramidal neurons. Mol Brain 5:11. https://doi.org/10.1186/1756-6606-5-11
38. Özgül C, Nazıroğlu M (2012) TRPM2 channel protective properties of N-acetylcysteine on cytosolic glutathione depletion dependent oxidative stress and Ca2+ influx in rat dorsal root ganglion. Physiol Behav 106(2):122–128. https://doi.org/10.1016/j.physbeh.2012.01.014
39. Nazıroğlu M, Özgül C, Çiğ B, Doğan S, Uğuz AC (2011) Glutathione modulates Ca(2+) influx and oxidative toxicity through TRPM2 channel in rat dorsal root ganglion neurons. J Membr Biol 242(3):109–118. https://doi.org/10.1007/s00232-011-9382-6
40. Lee M, Cho T, Jantaratnotai N, Wang YT, McGeer E, McGeer PL (2010) Depletion of GSH in glial cells induces neurotoxicity: relevance to aging and degenerative neurological diseases. FASEB J 24(7):2533–2545. https://doi.org/10.1096/fj.09-149997
41. Zhang J, Culp ML, Craver JG, Darley-Usmar V (2018) Mitochondrial function and autophagy: integrating proteotoxic, redox, and metabolic stress in Parkinson's disease. J Neurochem 144(6):691–709. https://doi.org/10.1111/jnc.14308
42. Mortadza SS, Sim JA, Stacey M, Jiang LH (2017) Signalling mechanisms mediating Zn(2+)-induced TRPM2 channel activation and cell death in microglial cells. Sci Rep 7:45032. https://doi.org/10.1038/srep45032
43. Moreno-García ME, Sumoza-Toledo A, Lund FE, Santos-Argumedo L (2005) Localization of CD38 in murine B lymphocytes to plasma but not intracellular membranes. Mol Immunol 42(6):703–711. https://doi.org/10.1016/j.molimm.2004.09.019
44. Jang Y, Lee MH, Lee J, Jung J, Lee SH, Yang DJ, Kim BW, Son H et al (2014) TRPM2 mediates the lysophosphatidic acid-induced neurite retraction in the developing brain. Pflugers Arch 466(10):1987–1998. https://doi.org/10.1007/s00424-013-1436-4
45. Togha M, Razeghi Jahromi S, Ghorbani Z, Ghaemi A, Rafiee P (2019) An investigation of oxidant/antioxidant balance in patients with migraine: a case-control study. BMC Neurol 19(1):323. https://doi.org/10.1186/s12883-019-1555-4
46. Tripathi GM, Kalita J, Misra UK (2018) A study of oxidative stress in migraine with special reference to prophylactic therapy. Int J Neurosci 128(4):318–324. https://doi.org/10.1080/00207454.2017.1374959
47. Chang JC, Lien CF, Lee WS, Chang HR, Hsu YC, Luo YP, Jeng JR, Hsieh JC, Yang KT (2019) Intermittent hypoxia prevents myocardial mitochondrial Ca^{2+} overload and cell death during ischemia/reperfusion: The role of reactive oxygen species. Cells 8(6):564. https://doi.org/10.3390/cells8060564
48. Espino J, Bejarano I, Paredes SD, Barriga C, Rodríguez AB, Pariente JA (2011) Protective effect of melatonin against human leukocyte apoptosis induced by intracellular calcium overload: relation with its antioxidant actions. J Pineal Res 51(2):195–206. https://doi.org/10.1111/j.1600-079X.2011.00876.x
49. Nazıroğlu M, Öz A, Yıldızhan K (2020) Selenium and neurological diseases: focus on peripheral pain and TRP channels. Curr Neuropharmacol 18(6):501–517. https://doi.org/10.2174/1570159X18666200106152631
50. Nazıroğlu M (2007) New molecular mechanisms on the activation of TRPM2 channels by oxidative stress and ADP-ribose. Neurochem Res 32(11):1990–2001
51. Perraud AL, Fleig A, Dunn CA, Bagley LA, Launay P, Schmitz C, Stokes AJ, Zhu Q et al (2011) ADP-ribose gating of the

calcium-permeable LTRPC2 channel revealed by Nudix motif homology. Nature 411(6837):595–599. https://doi.org/10.1038/35079100
52. Kraft R, Grimm C, Frenzel H, Harteneck C (2006) Inhibition of TRPM2 cation channels by N-(p-amylcinnamoyl)anthranilic acid. Br J Pharmacol 148(3):264–273
53. Togashi K, Inada H, Tominaga M (2008) Inhibition of the transient receptor potential cation channel TRPM2 by 2-aminoethoxydiphenyl borate (2-APB). Br J Pharmacol 153(6):1324–1330. https://doi.org/10.1038/sj.bjp.0707675
54. Vitoux MA, Kessal K, Melik Parsadaniantz S, Claret M, Guerin C, Baudouin C, Brignole-Baudouin F, Réaux-Le GA (2020) Benzalkonium chloride-induced direct and indirect toxicity on corneal epithelial and trigeminal neuronal cells: proinflammatory and apoptotic responses in vitro. Toxicol Lett 319:74–84. https://doi.org/10.1016/j.toxlet.2019.10.014
55. Yamamoto T, Mulpuri Y, Izraylev M, Li Q, Simonian M, Kramme C, Schmidt BL, Seltzman HH, Spigelman I (2021 Jan 29) (2021) Selective targeting of peripheral cannabinoid receptors prevents behavioral symptoms and sensitization of trigeminal neurons in mouse models of migraine and medication overuse headache. Pain. https://doi.org/10.1097/j.pain.0000000000002214
56. Liao CC, Li JM, Hsieh CL (2019) Auricular electrical stimulation alleviates headache through CGRP/COX-2/TRPV1/TRPA1 signaling pathways in a nitroglycerin-induced migraine rat model. Evid Based Complement Alternat Med 2019:2413919. https://doi.org/10.1155/2019/2413919
57. Morii A, Miyamura Y, Sago MI, Mizuhara M, Shikayama T, Naniwa M, Hitomi S, Ujihara I et al (2020) Orthodontic force-induced oxidative stress in the periodontal tissue and dental pulp elicits nociception via activation/sensitization of TRPA1 on nociceptive fibers. Free Radic Biol Med 147:175–186. https://doi.org/10.1016/j.freeradbiomed.2019.12.016
58. Karaaslan Z, Özçelik P, Ulukan Ç, Ulusoy C, Orhan KS, Orhan EK et al (2020) Plasma levels of inflammatory mediators in vestibular migraine. Int J Neurosci 130(4):330–335. https://doi.org/10.1080/00207454.2019.1681994
59. Franceschini A, Vilotti S, Ferrari MD, van den Maagdenberg AM, Nistri A, Fabbretti E (2013) TNFα levels and macrophages expression reflect an inflammatory potential of trigeminal ganglia in a mouse model of familial hemiplegic migraine. PLoS ONE 8(1):e52394. https://doi.org/10.1371/journal.pone.0052394
60. Kowalska M, Prendecki M, Kozubski W, Lianeri M, Dorszewska J (2016) Molecular factors in migraine. Oncotarget 7(31):50708–50718. https://doi.org/10.18632/oncotarget.9367
61. Güzel M, Nazıroğlu M, Akpınar O, Çınar R. (2021) Interferon gamma-mediated oxidative stress induces apoptosis, neuroinflammation, zinc ion influx, and TRPM2 channel activation in neuronal cell line: Modulator role of curcumin. inflammation. 2021 Apr 17. Epub ahead of print. https://doi.org/10.1007/s10753-021-01465-4.